Testing Approximations for Non–Linear Gravitational Clustering

Peter Coles[1,2],
Adrian. L. Melott[2], and **Sergei F. Shandarin**[2]

[1] *Astronomy Unit, School of Mathematical Sciences, Queen Mary & Westfield College, Mile End Road, London E1 4NS, UK*

[2] *Department of Physics and Astronomy, University of Kansas, Lawrence, Kansas 66045, U.S.A.*

Testing Approximations for Non–Linear Gravitational Clustering

Peter Coles[1,2], Adrian L. Melott[2], and Sergei F. Shandarin[2]

[1] *Astronomy Unit, School of Mathematical Sciences,*
Queen Mary & Westfield College, Mile End Road,
London E1 4NS, UK

[2] *Department of Physics and Astronomy,*
University of Kansas,
Lawrence, Kansas 66045, U.S.A.

April 27, 1992

Summary. We investigate the accuracy of various analytic approximations for following the evolution of cosmological density fluctuations into the non-linear regime. We compare the results of the application of linear theory, the lognormal approximation and the Zeldovich approximation to a set of initial data with corresponding results obtained by a full three-dimensional N-body computation from the same initial conditions. A cross-correlation technique is used to quantify the agreement between approximated and N-body "final" distributions for different initial power spectra, different normalisation epochs and different degrees of smoothing of the final results. We also studied the distribution function of mass density.

We find that the Zeldovich approximation is consistently the best approximation scheme. It is extremely accurate for power spectra characterised by $n \leq -1$; when the approximation is "enhanced" by truncating highly non-linear Fourier modes the approximation is excellent even for $n = +1$. It also matches the distribution function best of all our models, except at the high density tail where it fails to predict enough high-density regions. The performance of linear theory is less spectrum-dependent but this approximation is less accurate than Zeldovich for all cases because of the failure to treat dynamics. In fact, the truncated Zeldovich approximation is *always* more accurate than linear theory, even in the linear regime. The lognormal approximation provides generally a very poor fit to the spatial pattern, producing far too "clumpy" a distribution; on the other hand, the distribution of cell occupation densities *is* fitted reasonably well by a lognormal distribution, though not with the same variance as suggested by Coles & Jones (1991).

1 Introduction

Most theories of the origin of galaxies and large-scale structures in the Universe involve the assumption that such structures grew by gravitational instability from initially small fluctuations in the density of an almost homogeneous Universe. This assumption has recently received strong observational confirmation by the detection of temperature anistropies in the Cosmic Microwave Background Radiation (Smoot *et al.* 1992). The gravitational instability picture is easy to understand at the qualitative level since the only astrophysics it involves is gravity. Furthermore, when the density fluctuation amplitude is small compared to the mean density, the growth of fluctuations can be handled analytically using linear perturbation theory (e.g. Peebles 1980). However, galaxies and clusters of galaxies are clearly very non-linear objects today so we need to go beyond linear theory if we are to study the details of the structure formation process in these models.

The general problem of the evolution of clustering in the nonlinear case (i.e. when the clustering in strong) has proved to be analytically intractible in cases where the fluctuations are random (i.e. possess no special spatial symmetry). For the most part, cosmologists have therefore resorted to numerical techniques based on the N-body simulation to study the late stages of the evolution of density perturbations. In some cases, however, one needs to make more detailed predictions than can be obtained using such computational techniques. For this reason, various analytic approximations have been suggested to provide robust analytic results in certain circumstances. A good approximation can also furnish us with an understanding of the main processes involved in the formation of structure. For example the Zeldovich approximation, which we discuss below, describes the formation of "pancakes" and "filaments". The ability of this approximation to reproduce the final structures in different models can be related to the relative strength of the pancaking process in the development of clustering for the models.

In hierarchical clustering models, where structures form in a "bottom-up" fashion from small scales to large, one would expect linear theory to be a useful tool for probing very large-scale structure as long as one smooths out structures on small scales. This is usually expressed mathematically by smoothing or averaging the density on some length scale such that the smoothed density field then has *rms* fluctuations less than the mean density. But is this degree of smoothing sufficient to make linear theory accurate for a wide class of initial conditions? And how good is the agreement between such an application of linear theory and the actual non-linear density field?

One aspect of linear theory which is potentially disturbing is that the statistical distribution of the density field remains invariant under linear gravitational evolution, except for increasing variance. If the initial fluctuations have Gaussian statistics, as suggested by most inflationary theories (Guth & Pi 1982; Bardeen, Steinhardt & Turner 1983; Brandenberger 1985), then there is clearly a problem with the requirement that the density should be everywhere positive. As a simple corrective to this, Coles & Jones (1991) suggested the *Lognormal approximation* which essentially involves an exponential extrapolation of linear theory into the non-linear regime for which there is some empirical support (Coles & Jones 1991; Coles & Plionis 1991; Jones, Coles & Martínez 1992; Kofman *et al.* 1992a). But how good an approximation is the Lognormal distribution? Does it represent the distribution of non-linear clustering better than linear theory?

The main drawback with these two approximations is that they are effectively local; they simply involve mapping the initial density at some lagrangian co-ordinate to some function of that density at the same co-ordinate at some later time. In situations where structures have a predominantly *dynamical* origin involving large-scale motions of material, such local approximations must be poor representations of reality. In view of this inadequacy, Zeldovich (1970) introduced a *kinematic* approximation which uses the gravity-induced velocity field at eary times to map initial lagrangian co-ordinates onto non-linear Eulerian co-ordinates (Shandarin & Zeldovich 1989). The *Zeldovich approximation* has become a ubiquitous tool in analytical studies of clustering in models that involve pancake or "top-down" structure formation. But how good is the Zeldovich approximation in other circumstances? Is it better than linear theory for hierarchical models?

In this paper we shall investigate the above questions by performing a quantitative comparison of the density fields obtained by applying each of the above approximations with the density field obtained by a direct evolution of the (random) initial conditions using a three-dimensional N-body particle-mesh code. Throughout this work we shall assume a matter-dominated Universe with the closure density, i.e. $\Omega_0 = 1$. The quantitative comparison consists primarily of determining the point by point correlation coefficient between the N-body density and the approximated fields in a manner described more fully in section 4. All these approximations discussed in this paper are intended to deal with random initial mass distributions so we exclude, for example, extrapolations of linear theory based on the assumption of spherical symmetry. The layout of the paper is as follows: in Section 2, we describe the mathematical approximations we shall use and also such technicalities as smoothing; in Section 3 we describe briefly our ensemble of N-body experiments; in Section 4 we describe the cross-correlation procedure; results are discussed in Section 5 and the conclusions are presented in Section 6.

2 Evolution of Density Perturbations

The equations describing the evolution of density inhomogeneities in the expanding Universe under gravitational instability are as follows: first, define a dimensionless density contrast for the matter density $\rho(\underline{x})$ by

$$\delta(\underline{x}) = \frac{\rho(\underline{x}) - \rho_0}{\rho_0} \tag{1}$$

where ρ_0 is the mean matter density, and $\underline{x}$ are comoving co-ordinates: $\underline{x} = \underline{r}/a(t)$. We then have a system of three coupled non-linear partial differential equations: the *continuity equation*

$$\frac{\partial \rho}{\partial t} + 3H\rho + \frac{1}{a(t)}\underline{\nabla} \cdot (\rho \underline{v}) = 0; \tag{2}$$

the *Euler* equation

$$\frac{d\underline{v}}{dt} + H\underline{v} = -\frac{\underline{\nabla}\phi}{a(t)}; \tag{3}$$

and Poisson's equation

$$\nabla^2 \phi = 4\pi G \rho_0 a^2(t) \delta. \tag{4}$$

In these equations, $\underline{v}$ and ϕ are the peculiar velocity and peculiar gravitational potential respectively; $a(t)$ is the cosmological scale factor and, assuming a flat $\Omega_0 = 1$ Universe in the absence of pressure and radiation terms, $a(t) \propto t^{2/3}$ and $\rho_0(t) \propto a^{-3} \propto t^{-2}$. The Hubble expansion parameter, $H = (\dot{a}/a)$.

In order to solve these equations, we need to specify some initial data. In this study, we shall assume a scale-free initial power spectrum of density perturbations:

$$P(k) = \langle |\delta_k|^2 \rangle \propto k^n, \tag{5}$$

where δ_k is the spatial Fourier transform of the density contrast (1). We shall take $n = -2, -1, 0, +1$ as illustrative examples in this paper. (Actually, we shall discuss the case $n = -1$ in more detail later in the paper as we feel it is the most relevant scale-free spectrum for gravitational clustering). We assume further that, at some initial time t_i where we define $a(t_i) = 1$ the density contrast is small and the phases of the Fourier components are randomly distributed on the interval $[0, 2\pi]$. This is sufficient to guarantee that $\delta(\underline{x})$ is a Gaussian random field: all its statistical properties are then completely determined by $P(k)$.

The simplest approximate solution to the system (1)–(5) is obtained from *linear perturbation theory* (e.g. Peebles 1980). By writing $\rho = \rho_0(1 + \delta)$ and solving the system (1-5) to first order in δ, we find the solution for the growing perturbation mode to be:

$$\delta(\underline{x}, t) = \frac{2\nabla^2 \phi}{3H^2 a^2}. \tag{6}$$

Since $H^2 \propto a^{-3}$ for a matter-dominated Universe with the closure density and $\phi(\underline{x})$ is constant to first order in perturbation theory, we have

$$\delta(\underline{x}, t) = a(t)\delta(\underline{x}, t_i) \tag{7}$$

so that $P(k) \propto a^2$ in linear theory. The statistical distribution of δ therefore remains constant, except for a scaling of the variance. Note that this solution is *local*, in that $\delta(\underline{x}, t)$ depends only upon the

$\delta(\underline{x}, t_i)$ at the same spatial co-ordinate at earlier times. Furthermore, it is clear that the solution (7) must be invalid with Gaussian initial data when $\sigma^2 \equiv \langle\delta^2\rangle \sim 1$, since the Gaussian distribution assigns a non-zero probability to regions having $\delta < -1$ in such a case (e.g. Fry 1985).

We can make a crude correction to this by defining a *chopped* linear field by

$$\delta(\underline{x}, t) = \begin{cases} \alpha_1(t)[1 + a(t)\delta(\underline{x}, t_i)] - 1 & \delta(\underline{x}, t) \geq -1 \\ -1 & \text{otherwise} \end{cases} \tag{8}$$

where $\alpha_1(t)$ is a "renormalising" factor introduced to keep the mean density of the Universe constant, i.e. $\langle\delta\rangle = 0$.

A further improvement upon simple linear theory was suggested by Coles & Jones (1991): *the Lognormal Model.* Here the condition that $\delta \geq -1$ is met by choosing a different local mapping:

$$\delta(\underline{x}, t) = \alpha_2(t)\exp[a(t)\delta(\underline{x}, t_i)] - 1. \tag{9}$$

the renormalising factor is now $\alpha_2(t) = \exp(-\sigma^2 a^2/2)$. We see from (9) that, to first order in δ, the lognormal model matches linear theory (7). Arguments for the appropriateness of this approximation for gravitational clustering in the non-linear regime are given by Coles & Jones (1991), Coles & Frenk (1991), Jones *et al.* (1992) and Kofman *et al.* (1992a). Note also that the three approximations (7), (8) & (9) are all local in the sense described above and one might therefore doubt their ability to trace accurately structures developed on very small scales by highly non-linear interactions; matter moves great distances away from its initial Lagrangian position when clustering is strong. We might therefore expect small-scale clustering predicted by these approximations to be incorrect and that better approximations might be achieved by attempting only to follow long wavelength perturbation modes. To check this out, we introduce *truncated* linear and lognormal approximations obtained by extrapolating not the full linear density field as in (7) & (9), but the field obtained by filtering out small-scale highly non-linear modes. (We find the chopped linear theory behaves almost identically to the straightforward linear theory so we do not discuss the filtered version of this model.) We choose a sharp k-space cutoff for this purpose. Define a k-space truncated field by:

$$\delta_{k_*}(\underline{k}, t_i;\, k_*) = \begin{cases} \delta_k(\underline{k}, t_i) & |\underline{k}| \leq k_* \\ 0 & \text{otherwise.} \end{cases} \tag{10}$$

The resultant real-space field denoted $\delta^*(\underline{x}, t_i)$ is then used to obtain the extrapolated results:

$$\delta(\underline{x}, t) = a(t)\delta^*(\underline{x}, t_i) \tag{11}$$

and

$$\delta(\underline{x}, t) = \alpha_2(t)\exp[a\delta^*(\underline{x}, t_i)] - 1, \tag{12}$$

by analogy with (7) and (9) respectively. The scaling parameter α_2 is, of course, different to that defined in (9).

An appropriate scale for performing this k-space truncation is around the wavenumber corresponding to the transition into non-linear evolution: k_{nl}, defined by:

$$a^2(t)\int_0^{k_{nl}} P(k)d^3\underline{k} = 1, \tag{13}$$

where clearly k_{nl} decreases with t as successively larger scales enter the non-linear regime.

A qualitatively different approximation which attempts to track the displacement of matter particles away from there initial Lagrangian positions is the Zeldovich approximation (Zeldovich 1970). Here one makes an *ansatz* relating the Eulerian (comoving) co-ordinates of a matter point, $\underline{x}$, at some time t to the initial unperturbed Lagrangian co-ordinates $\underline{q}$.

$$\underline{x}(\underline{q}, t) = \underline{q} + a(t)\underline{\nabla}\Phi_i(\underline{q}) \tag{14}$$

where $\Phi_i(\underline{q})$ is the initial *velocity potential*, related to the initial peculiar gravitational potential by

$$\phi_i(\underline{x}) = -\frac{3}{2}H^2 a^3 \Phi_i(\underline{x}). \tag{15}$$

Here the spatial structure of the nonlinear density field is determined by the inverse of the determinant of the deformation tensor, $S_{ij} = \delta_{ij} + a\frac{\partial^2\Phi_0}{\partial q_i \partial q_j}$. At the epoch defined by the scale factor a_c, in the vicinity of the Lagrangian point $\underline{q}_c$, the density formally reaches infinity when the leading eigenvalue of S_{ij} reaches $\lambda_1(\underline{q}) = 1/a_c$; this phenomenon is known as shell-crossing and it indicates the transition from single-stream into multi-stream flow (Shandarin & Zeldovich 1989). The *ansatz* (14) breaks down at this point as trajectories cross. Until this catastrophe is reached, however, the Zeldovich approximation does track the motion of material fairly well and we would expect it to be a better approximation to the actual density distribution than the local approximations (7)–(12) for initial power-spectra that do not predict excessive shell-crossing on small scales. Traditionally the Zeldovich approximation is assumed to be good only when long-wavelength perturbation modes dominate which is sometimes formally expressed as $n \leq -3$. We would expect spectra with any significant large-scale power (e.g. $n = -1, -2$ in (5)) also to fall into this category. However, in the same spirit as that which motivated the k-space truncated *local* approximations (11) & (12), we can expect to improve upon the simple Zeldovich approximation (14) by removing initial power in waves with $k > k_{nl}$. We shall refer to such an approximation as a *truncated* Zeldovich approximation (first suggested by Kofman *et al.* 1992b).

3 Numerical Simulations

To provide comparison data sets for testing these approximation schemes we perform numerical N-body experiments to follow the evolution of a cosmological density field approximated by a set of particles on a grid. The simulations used are described in much more detail elsewhere so we provide only essentials.

To obtain generic results we use power-law density fluctuations of the form (5) as initial conditions. These fluctuations are of very low amplitude and are imposed by Fourier Transform on an array of particles on a uniform cubic lattice. At very low amplitude our use of the Zeldovich approximation (14) for initial conditions generates not only particle displacements but also velocities in accord with the growing mode of gravitational instability. Our initial conditions were generated with the amplitude restriction that no particle can move more than 1/2 the cell width in response to the initial perturbations.

In this study we examine simulations with 128^3 particles, each on a comoving 128^3 mesh with periodic boundary conditions. We used the enhanced PM (particle–mesh) method of Melott (1986). This makes them resolution-equivalent to simulations with 128^3 particles on a 256^3 grid in traditional PM codes; see also Park (1992, preprint) and Weinberg *et al.* (1992, *in preparation*). The simulations

were run for various expansion factors $a(t)$, normalised by k_{nl} as defined by (13). We studied spectra corresponding to $n = 1, 0, -1, -2$ (three realisations each), for $k_{nl} = 8k_f$ and $4k_f$, where k_f is the fundamental mode of the box. These two scales represent a good compromise between resolution in terms of particles which drives one to look at large scales and the effect of our periodic boundary conditions which leads one towards smaller scales (Kauffmann & Melott 1992). To give some idea of the visual appearance of the full N-body results we display, in Figures 1 & 2, slices through the final particle distributions for $k_{nl} = 8$ and $k_{nl} = 4$ respectively. Notice the strong impression of "filamentarity" in the cases where $n =\leq -1$ but that this impression is transient: as k_{nl} decreases, the tendency of the structure to clump on small scales dominates the pattern. A general increase in clustering strength is clearly discernible in all cases for $k_{nl} = 4$ rather than $k_{nl} = 8$. The visual impressions of the spatial structures in the different simulations are similar because we use the same set of (random) phases for all spectra; we shall discuss these visual impressions in much more detail in Section 5.

FIGURES 1 & 2

Since our particles began on a regular cubic lattice, and since we are uniformly sampling alternate particles in each direction (i.e. 1/8 of the particles altogether) to make the plots, the reader can easily discern relics of the lattice in the extremely low-density regions in those cases where there is little power on small scales. Our actual particle density is much higher, but plotting limitations prevent us from showing them all. We could eliminate the lattice appearance by random rather than uniform sampling, but that would introduce a shot-noise error into the pictures. At our actual computational particle density the lattice has little effect on dynamics. For example, we can reproduce analytic results for spherically-symmetric collapse and void expansion very well (Peebles *et al.* 1989), in spite of the cubic symmetry of our code.

To suppress any shot noise effects in our quantitative analysis we binned the resulting particle distribution into densities on a 64^3 mesh. Further Gaussian smoothing, as described later, was allowed to vary so that we could study the results at various density contrasts. To compare these distributions directly with the density distributions obtained from the approximations introduced in section 2, we also binned the initial (linear) fluctuations onto 64^3 grids and mapped them point-by-point into the "final" distributions using (7)–(12).

Zeldovich results were created by evolving the initial data (with and without k-space truncation) by the Zeldovich approximation (14) on the 128^3 mesh and then binning onto 64^3 grids at the end, as in the N-body result. Since the Zeldovich approximation is the only one of our examples that actually produces a point distribution, we have plotted diagrams analagous to those of Figures 1 and 2, but for brevity we display in Figure 3a,b only the case where $n = -1$ and only for truncated initial spectra. These plots should be compared with Figure 1c and 2c respectively. Notice how the the Zeldovich approximation seems, qualitatively at least, to produce a similar large-scale distribution although the small-scale structures are clearly different in the N-body case. Notice further how the extensive shell-crossing that occurs when $k_{nl} = 4$ results in a washing out of the structures; a similar phenomenon occurs at a much earlier epoch for $n > -1$ which is why we introduced the k-space truncation in Section 2. The relics of the initial grid are also clearly apparent in the Zeldovich figures, even more so than in the N-body case because of the failure of the Zeldovich approximation to include small-scale forces.

FIGURE 3

Because we extrapolate only the smoothed density field using our other approximation schemes (7)-(12), we cannot make plots of this kind for them. In order to construct a visual representation of the distributions obtained from *all* of our approximation schemes, we therefore need to represent a continuous distribution. The simplest way to do this is to produce a grey-scale plot. Figure 4 consists of 7 grey-scale plots showing N-body, Zeldovich (truncated and untruncated), linear theory (truncated and untruncated) and lognormal (truncated and untruncated). The linear grey scale is applied to regions with $1 < \delta < 10$; regions with $\delta < 1$ appear white, regions with $\delta > 10$ appear black. The example shown has $n = -1$ and $k_{nl} = 8$; this example is representative of the general performance of the different approximations, as we shall see in the next section.

FIGURE 4

Qualitatively, both the Zeldovich variants produce a pattern similar to the N-body distribution on large scales but do not trace the small-scale structure well. The untruncated Zeldovich approximation has a washed-out appearance because of the copious shell-crossing, even at $k_{nl} = 8$. Both linear and lognormal untruncated seem to bear very little resemblance to the N-body result, although in the linear case at least, some of the densest regions are in roughly similar positions (e.g. the two dense concentrations at top right). The lognormal distribution clearly produces too few concentrations and those that are produced a far too dense; there is, however, some spatial resemblance between the positions of the dense regions in the model and N-body distributions. The truncated linear and lognormal distributions are very similar but both seem to bear only a vague resemblance to the final N-body distribution. Clearly the final structures in such a model have been much influenced by dynamics in their formation, which is not well described by local approximations. It is incidental to the main purpose of this work, but this clearly casts doubt on treatments of galaxy clustering that rely upon the identification of peaks in the linear density field with non-linear objects at late times (e.g. Bardeen *et al.* 1986): there seems to be very little spatial correspondence between linear and non-linear fields which has already been demonstrated in the case of one-dimensional gravity (Williams *et al.* 1991).

4 Cross-Correlations

Interesting though the visual impressions gleaned from Figures 1 to 4 may be, we clearly need some way to measure objectively how well the N-body results compare, not just with the Zeldovich approximation but also with our other analytical models (7)–(12). The main tool we use to check the accuracy of the analytic approximations we discussed above is quite simple. Basically, we compare each grid-point in the density field evolved by the approximation schemes with the corresponding grid-point for the full numerical solution. To quantify the correspondence between the two fields, we compute the product-moment correlation coefficient:

$$S_{XY} = \frac{\langle (X_i - \bar{X})(Y_i - \bar{Y}) \rangle}{\langle (X_i - \bar{X})^2 \rangle^{1/2} \langle (Y_i - \bar{Y})^2 \rangle^{1/2}} \tag{16}$$

where X_i, Y_i represent the density contrasts in the i-th pixel of the N-body and model distributions respectively, and averages are taken over all pixels in the simulations. Note that $|S| \leq 1$ and a value $S = +1$ denotes perfect agreement between each point in X and each point in Y though it does not imply that $X = Y$ at every pixel, eg. $X = CY$ with C constant obviously also gives $S = +1$. The

variance of X and Y scale out of this problem so one can get a perfect correlation coefficient even if the variance is not the same for the two distributions as long as there is a good spatial correspondence between the two distributions. If the structures in the two distributions are in the same place, however, but the distribution functions are different, the correlation coefficient will, in general, be less than unity.

We should point out at the start however that such a point-by-point test is a very severe test for *any* approximation scheme, especially if the density field is strongly non-linear on some scale. The approximated spatial structure might be quite similar to the N-body results in terms of relative position of the main features, but if the inhomogeneities are in just slightly the wrong position in the model field compared to the N-body field, a very weak correlation coefficient will be obtained. To relax the test we therefore compute not just for the "raw" density fields but also for fields obtained by smoothing the density field on some scale R. We smooth both N-body and approximated fields:

$$\delta(\underline{x}, R) = \int d^3\underline{x}'\, \delta(\underline{x}') W(|\underline{x} - \underline{x}'|; R) \tag{17}$$

we have chosen, for convenience, a Gaussian window function W:

$$W(|\underline{r}|; R) = \frac{1}{\sqrt{2\pi} R} \exp\left(-\frac{r^2}{2R^2}\right) \tag{18}$$

Roughly speaking, one expects linear theory and the other approximations to be valid perhaps until $\sigma^2(R) = \langle \delta(\underline{x}, r)^2 \rangle = 1$ or until clustering defined by the two-point correlation function, $\xi(r)$, has an amplitude greater than unity. To determine more rigorously the point where these approximations begin to fail, we examine smoothing scales around the *correlation scale*, r_c, defined by $\xi(r_c) = 1$. This scale is related to the reciprocal of k_{nl} in a spectrum-dependent fashion (Melott & Shandarin 1992). We shall find it convenient in the next section to give S as a function of σ rather than R so that the computer grid scale does not appear in the plots). For information, we show in Figure 5 how the rms fluctuation $\sigma(R)$ scales with the filter radius R for $k_{nl} = 4$ and $k_{nl} = 8$ for each of the 4 test power spectra. Note that the rms fluctuation increases at a fixed smoothing scale as k_{nl} decreases.

FIGURE 5

5 Results and Discussion

We actually ran 3 different realisations of each of the 4 initial power spectra; each of these 12 produces, at a given expansion factor, 7 distributions [N-body; linear (7); "chopped" linear (8); lognormal (9); truncated linear (11); truncated lognormal (12)]. The two different values of k_{nl} correspond to 2 different scale factors. The total number of distributions we cross-correlated therefore is 168, and we study the behaviour of S for each as a function of $\sigma(R)$.

The set of 3 different random-phase realisations of the initial conditions allows one to estimate the errors in S for a given model; the typical errors we obtained were of order 10^{-3} in S so we do not plot these on the figures we shall show in this section. The value of S does indeed seem to be a reliable indicator of the performance of each of these models.

Figure 6a,b,c,d shows the behaviour of the the cross-correlation coefficient S as a function of σ for all the approximations and for the 4 different initial power spectra. Some points are immediately noticeable.

FIGURE 6a,b,c,d

First, all models become more and more accurate as σ is decreased (i.e. as the smoothing scale increases). The only exception to this rule is the chopped linear model and then only for $n = +1$. The reason for this is that the "chopping" process is applied to the linear field before smoothing; the chopping and smoothing do not commute and the resulting smoothed distribution will always be incorrect in the underdense regions. This is not such a problem for $n < 1$ because the linear density field in these cases does not have *rms* amplitude much greater than unity even without smoothing in these other cases.

Second, note that while the curves for $k_{nl} = 4$ and $k_{nl} = 8$ are not identical for the same power spectrum, the relative performance of the different models is independent of the normalisation. The main reason for checking the two different normalisations was to see if the results do behave in a scale-free manner as expected from the scale-free initial conditions and the scale-free nature of gravity. The finite spatial and frequency resolution of the code we use obviously destroys this invariance at very small and very large scales but that is clearly not a problem for the two normalisations we have chosen for this work. The exact value of S thus obtained depends on how well individual structures are resolved, which depends on k_{nl}, but the relative values for the different approximations do not.

The other immediately obvious point is that all approximations become less accurate (i.e. S increases) at a given σ as n increases. This is because the relative amounts of small-scale clustering compared with large-scale clustering increases in these cases. We expect all of our approximations to have problems when there is lots of small scale power.

Now let us consider each kind of approximation in turn.

The (untruncated) Zeldovich approximation performs poorly for $n = +1$, unless the field is heavily smoothed ($\sigma \ll 1$). Its performance is slightly worse for $k_{nl} = 4$ compared to $k_{nl} = 8$ for all spectra (there is more shell-crossing the smaller k_{nl}). The approximation is, however, extremely good for $n \leq -1$ even when σ is of order unity and beyond. The dramatic improvement obtained by *truncating* the small-scale modes at k_{nl} even for $n = +1$ is remarkable. After such a truncation, the Zeldovich approximation is significantly better than linear theory in the mildly non-linear regime. In most cases, it is significantly better than linear theory even in the linear regime. Interestingly, however, the truncated Zeldovich approximation is actually worse than the untruncated approximation for $n = -2$ in the non-linear regime. This must be because there is little small-scale structure in this case and the simple Zeldovich approximation can follow a small amount of small-scale clustering reasonably accurately. Removing the small-scale structure therefore reduces the performance of the approximation. It is important to stress that this cannot be connected with a cutoff of the spectrum at the Nyquist frequency: the stages we discuss have k_{nl} respectively 8 and 16 times smaller than the Nyquist frequency in the initial conditions. On the other hand, when there is a lot of small-scale power (as in $n = +1$) Zeldovich gets small-scale structure all wrong and the approximation is improved by removing the small-scale structure altogether.

The performance of linear theory is much less spectrum-dependent. The shapes of the curves of S versus σ are remarkably similar for all power spectra, although the gap in performance between linear theory and the Zeldovich approximation increases as n decreases. In no case does the "chopped" linear theory improve upon the straightforward application of (7) so we shall not discuss this model further. Truncated linear theory also performs less well, in all cases, than the straightforward version. This confirms the comments in Section 3 about the visual impression of the agreement between linear theory and the N-body results: even with heavy smoothing the N-body results do not trace the linear

structures at all well. Of course the k-space truncation corresponds to a smoothing in real space so even effectively smoothing twice does not bring about a good agreement.

The straightforward lognormal approximation (9) is extremely poor even with heavy smoothing. Indeed for the cases with $k_{nl} = 4$ it was not possible to compute the lognormal approximation because of arithmetic overflows occuring when the exponentiation in (9) was attempted. Any small-scale non-linear structure causes this approximation to have problems; the mapping (9) is just too steep. There is, however, some improvement with decreasing spectral index. The truncated lognormal approximation is better, but still not as good as linear theory, producing a performance roughly comparable to – and indeed, in some cases almost exactly the same as – linear theory.

To reinforce the main points we have made, Figure 7 shows the linear theory and truncated Zeldovich results for all the power spectra plotted on the same graphs. Notice how the performance of linear theory versus σ is almost spectrum–independent and scales roughly with k_{nl} (less accurately so for the more negative power-spectra). The Zeldovich results also scale roughly for a given power-spectrum, but are more dependent upon the initial spectrum. One can interpret this as a relative increase in the importance of "pancaking" in gravitational clustering with decreasing n. Nevertheless, the truncated Zeldovich result is *always* better than linear theory, even when $n = +1$, a situation when this approximation is rarely applied. Extrapolating this result to cases where $n > +1$ leads us to speculate that it is only when $n > +1$ that pancaking is unimportant for gravitational clustering.

FIGURE 7

Aside from the visual "calibration" provided particularly by Figure 4, it is difficult to assign a meaning to the actual numerical value of S for any particular situation. We discussed above the possibility that, without smoothing, only a slight displacement of structures in the N-body and model results could result in a low value of S even if the spatial patterns produced in the two cases were quite similar. In order to understand how S increases with smoothing scale in such a case, consider the following toy example. Suppose we have a density distribution in one dimension represented by a single point mass. Now construct another distribution by displacing the mass by a distance d (representing the mis-match between model and N-body result). We now smooth each distribution by Fourier convolution with a Gaussian filter of width R and compute the cross-covariance between the two distributions. The result is simply calculated: $S = \exp(-d^2/4R^2)$ (the actual values of the two masses scales out of the problem). In this case if $R = d$, $S \simeq 0.8$. Smoothing by the correlation scale typically produces an S of this order for linear theory (see Figure 5) and this might be interpreted, roughly speaking, as meaning that the largest structures are typically misplaced by a distance of order the correlation length in linear theory relative to the real distribution. The situation is of course more complicated than this in three dimensions because the behaviour of S with R will then be strongly dependent upon the geometry of the mass distributions in the two cases.

It is worth also pointing out that the procedure of k-space truncation actually produces a density field which has a calculable correlation coefficient with respect to the original field. If we take linear theory as an example, we find that the cross correlation coefficient is given by

$$S = \sqrt{\frac{\int_0^{k_{nl}} P(k)k^2 dk}{\int_0^{\infty} P(k)k^2 dk}}. \tag{19}$$

Unfortunately the lower integral diverges for power-law spectra but, for our simulations anyway, the power-spectrum is truncated at the Nyquist frequency of the 128^3 grid: $k_N = 64$. Taking this as the

upper limit of integration in the denominator we get

$$S = \left(\frac{k_{nl}}{k_N}\right)^{(n+3)/2} . \tag{20}$$

For $n = -1$ and $k_{nl} = 8$ (i.e., 16 in units of the 128^3 grid) this gives $S = 0.25$. This gives some idea of the measure of correlation one can expect by just removing high-frequency power from the density field, i.e. just ignoring small-scale features.

Of course, the cross-correlation coefficient is just a single number for each of the simulations and one cannot hope to represent all the detailed relative behaviour of the different approximations in a single number. To give some more information about some of our results we have plotted, in Figure 8, scatter diagrams of the cell density (actually, $1 + \delta$) in the N-body results against that in the model results for selected power spectra (just $n = 1, -1$), for two diffferent smoothing scales, $R = R_c$ and $2R_c$, and just for the truncated Zeldovich, linear and truncated lognormal approximations. These examples greatly elucidate the reason for the relative performance of the models, and also give the reader a means of visually interpreting the quantitative value of S.

FIGURE 8

Notice how smoothing considerably tightens the relationships, as expected. There is considerable scatter in the Zeldovich results for $n = 1$ but the relationship is clearly better than linear theory. Whereas linear theory looks roughly the same for $n = -1$ at the same smoothing scale, the Zeldovich approximation is clearly better. When the smoothing scale is $2R_c$, where R_c is the correlation length, the relationship is very tight indeed, but there is clearly still a systematic deviation: both very high and very low densities are incorrectly predicted by the Zeldovich approximation. The systematic effect is gross for the linear results in this case, particularly in the low-density regions.

We see also reasons for the poor performance of the lognormal approximation: the k-space truncation is too severe, reducing the fluctuations too much compared to the "real" results. However, the fact that the lognormal result smoothed at $2R_c$ has less systematic deviation than linear theory suggests that some other truncation criteria might produce a fairly good approximation.

The generally disappointing performance of the lognormal model casts doubt upon the argument for it outlined by Coles & Jones (1991). But there is considerable evidence that the distribution function of galaxy counts is approximately lognormal, both in 3-d space and projection, and there is some evidence for lognormality in the multifractal description of galaxy clustering (Coles & Jones 1991; Coles & Plionis 1991; Coles & Frenk 1991; Jones *et al.* 1992; Kofman *et al.* 1992a). We have, however, here chosen to implement a specific lognormal model which produces a final distribution function whose variance is fixed by the linear density fluctuation amplitude. This study has shown that this procedure, based on crude kinematical considerations, is not an accurate procedure in general. However, this does not mean that the distribution function can not be accurately represented by a lognormal distribution. In Figure 9, we plot the distribution functions for a representative example of our simulations ($k_{nl} = 8$; $n = -1$; $R = R_c$).

FIGURE 9

The first noticeable feature of the N-body distribution function is that it possesses a long tail, approximately of straight line form in this plot. This is very characteristic of lognormal distributions

(Kofman *et al.* 1992a give other examples); but it should be stressed that smoothing and exponentiating the linear field (9) do not commute: our lognormal approximation does not produce distribution functions after smoothing that are themselves exactly lognormal. The untruncated lognormal distribution (left) gives too extended a tail, whereas the truncated lognormal has too shallow a tail. Given freedom to match the variance (equivalent to choosing different truncation wave-numbers) a lognormal distribution would clearly provide a good fit to the distribution function. To summarise, our lognormal approximation (9) & (12) reproduces neither the spatial structure nor distribution function of the real non-linear distribution very well at late times, but the distribution function does seem to be fit by a lognormal distribution of some kind; this question is discussed further in Jones *et al.* (1992) and Kofman *et al.* (1992a).

It is interesting also to note that the untruncated Zeldovich approximation matches the distribution function at moderate and low densities, but fails in the high-density regions by not producing enough very dense regions. This is clearly a consequence of the failure to treat small-scale interactions correctly as the orbits begin to intersect. Notwithstanding this problem, the truncated Zeldovich approximation provides the best fit to the distribution function of all those we have tried. For $n = -1$ and $k_{nl} = 8$, it is almost indistinguishable from the N-body results if $\rho \leq 3.5\rho_0$.

6 Conclusions

We have systematically and quantitatively compared various analytic approximations for non-linear gravitational clustering with the results of "full" N-body simulations. The cross-correlation coefficient is a simple and easy to interpret method for comparing two spatial distributions; we have used it to determine the degree of correspondence between approximations and N-body results as a function of the degree of smoothing. We have probed a wide range of initial power spectra and have checked that our results are not influenced by resolution or boundary effects.

In terms of both visual resemblance and cross-correlation coefficient the Zeldovich approximation is the best of our schemes and, in its k-space truncated form, it is surprisingly accurate even for initial power spectra with lots of small-scale power. The Zeldovich approximation in this form is *always* better than linear theory (it is even better in the linear regime), although the efficacy of linear theory in absolute terms is much less dependent upon the initial power spectrum than is the Zeldovich approximation. The considerable improvement of the Zeldovich approximation can be interpreted as the relative increase of "pancaking" in gravitational clustering with decreasing n. It is also important to stress that we have discussed the domain where $n > -3$ where the performance of the Zeldovich approximation has often been assumed to be very poor (e.g. Peebles 1980). Knowing that the Zeldovich approximation describes the formation of pancakes we conclude that pancaking is important not only in its traditional domain of spectra with sharp cutoffs or power-laws with $n < -3$ at the beginning of the non-linear stage, or even for $n < -1$ as the adhesion model suggests (Kofman *et al.* 1992b and references therein) but that it is an important process for all power-law spectra with $n < +1$. Certainly the Zeldovich approximation (which includes pancake formation) is a much better approximation for the nonlinear stages in such cases than a simple extrapolation of linear theory. In other words the degree to which filaments and sheets are present in the results of N-body simulations is directly related to the performance of the Zeldovich approximation. Our present results prove that the Zeldovich approximation is very good if $n < -1$ and deteriorates with increasing n. Of course one has to keep in mind that all results were obtained for initial power-spectra in the finite range between the fundamental

mode $k_f = 1$ and the Nyquist mode $k_N = 64$. A direct extrapolation of these results to pure power-law spectra on the infinite range $0 < k < \infty$ can be dangerous without a clear understanding of how to make the transition the limit $k_N/k_f \to \infty$.

We see the importance of this result for cosmology as explaining the large-scale structure of the Universe as a result of gravitational clustering from initial conditions without a sharp cutoff on the scale of tens of Mpc. The slope of the initial spectrum is, however, probably negative on the scales of clusters and superclusters ($n \sim -1$) in good agreement with early suggestions. An example of a spectrum with such a form is given by the CDM model (Bardeen *et al.* 1986).

It is worth stressing that we tested only the simplest naive extrapolation of linear theory. If more elaborate extrapolation schemes are assumed they cannot be rigorously verified on the basis of the present results but our results strongly suggest that one should test the validity of any such extension of linear theory before using it to speculate about cosmology.

The lognormal approximation – the form of the lognormal distribution suggested by Coles & Jones (1991) – performs badly relative to both linear and Zeldovich approximations in terms of producing the same spatial structure and does not match the density distribution function at all well. On the other hand, from this study and other related works (Jones *et al.* 1992; Kofman *et al.* 1992a) there is now considerable evidence that gravitational clustering is well described by a lognormal distribution function. One must conclude therefore that although the lognormal distribution may be correct, the attempt to provide a motivation for it by extrapolating linear theory through the continuity equation was incorrect and some other physical motivation must be sought.

Acknowledgments. We thank the University of Kansas for the short-term visiting professor program which made this work possible. We are grateful for research support from NASA grant NAGW 2923 and NSF grant AST–9021414 and a block of Cray-2 time at the National Center for Supercomputing Applications. We thank A. Klypin and R. Splinter for assistance with graphics and Lev Kofman for discussions and for suggesting the scatter diagrams to us.

References

Bardeen, J.M., Bond, J.R., Kaiser, N. & Szalay, A.S., 1986. *Astrophys. J.*, **304**, 15.

Bardeen, J.M., Steinhardt, P.J. & Turner, M.S., 1983. *Phys. Rev. D*, **28**, 679.

Brandenberger, R.H., 1985. *Rev. Mod. Phys.*, **57**, 1.

Coles, P. & Barrow, J.D., 1987. *Mon. Not. R. astr. Soc.*, **228**, 407.

Coles, P. & Frenk, C.S., 1991. *Mon. Not. R. astr. Soc.*, **253**, 727.

Coles, P. & Jones, B.J.T., 1991. *Mon. Not. R. astr. Soc.*, **248**, 1.

Coles, P. & Plionis, M., 1991. *Mon. Not. R. astr. Soc.*, **250**, 75.

Fry, J.N., 1985. *Astrophys. J.*, **289**, 10.

Guth, A.H. & Pi, S-Y., 1982. *Phys. Rev. Lett.*, **49**, 1110.

Jones, B.J.T, Coles, P. & Martínez, V.J., 1992. *Mon. Not. R. astr. Soc., in press.*

Kauffmann, G. & Melott, A.L., 1992. *Astrophys. J.*, **000**, 000.

Kofman, L., Gelb, J., Bertschinger, E., Nusser, A. & Dekel, A., 1992a. *Preprint.*

Kofman, L., Pogosyan, D., Shandarin, S.F. & Melott, A.L., 1992b. *Astrophys. J.*, **000**, 000.

Melott, A.L., 1986. *Phys. Rev. Lett.*, **56**, 1992.

Melott, A.L. & Shandarin, S.F., 1992. *In Prep.*

Peebles, P.J.E., 1980. *The Large-scale Structure of the Universe*, Princeton University Press, Princeton.

Peebles, P.J.E., Melott, A.L., Holmes, M.R. & Jiang, L.R., 1989. *Astrophys. J.*, **345**, 108.

Shandarin, S.F. & Zeldovich, Ya. B., 1970. *Rev. Mod. Phys.*, **61**, 185.

Smoot, G.F. *et al.* 1992. *Astrophys. J. Lett., submitted.*

Williams, B.G., Heavens, A.F., Peacock, J.A. & Shandarin, S.F., 1991. *Mon. Not. R. astr. Soc.*, **250**, 458.

Wright, E.L. *et al.*, 1992. *Astrophys. J. Lett., submitted.*

Zeldovich, Ya. B., 1970. *Astron. Astrophys.*, **5**, 84.

Figure Captions

Figure 1. Positions of every second particle in a slice two cells thick in our final N-body simulations. The figures have the same (random) phases but different spectra, as labelled by the different values of n. The normalisation corresponds to $k_{nl} = 8$.

Figure 2. As Fig. 1, but with $k_{nl} = 4$.

Figure 3. Dot-plots of slices through the distributions obtained by evolving the same initial conditions as Figure 1,2 by the truncated Zeldovich approximation until $k_{nl} = 8$ (left) and $k_{nl} = 4$ (right) for the case $n = -1$; these should be compared with the bottom left parts of Figs 1 & 2 respectively.

Figure 4. Grey-scale plots of (a) N-body (b) Zeldovich (c) truncated Zeldovich (d) linear (e) truncated linear (f) lognormal (g) truncated lognormal. The plots represent on a linear grey-scale densities between $10 > \delta > 1$. Regions with $\delta < 1$ appear white; those with $\delta > 10$ appear black. The initial power spectrum is $n = -1$ and $k_{nl} = 8$; the N-body and Zeldovich results can be compared directly to Figures 1 and 3.

Figure 5. Behaviour of the *rms* density fluctuation in our N-body simulations as a function of smoothing scale (in computer grid units) for our different power spectra and normalisations.

Figure 6a,b,c,d. Plots of cross-correlation coefficient, S against rms density fluctuation σ for (a) $n = 1$, (b) $n = 0$, (c) $n = -1$ and (d) $n = -2$. The left plot of each pair has $k_{nl} = 8$, the right has $k_{nl} = 4$. The different models are indicated on the key: Z (Zeldovich); O (lognormal); L (linear). The k-space truncation is labelled as (t) and the chopped linear theory (8) is labelled $L(c)$. the lognormal does not appear in some cases because of overflow errors (see text).

Figure 7. Summary of the results for linear theory (left) and truncated Zeldovich (right) for all power spectra and for $k_{nl} = 4$ (lines only) and $k_{nl} = 8$ (lines connecting open circles).

Figure 8. Scatter plots of approximate results vs N-body results for selected cases. The three rows correspond to (top) truncated Zeldovich (middle) linear theory (bottom) truncated lognormal. From left to right in each row we have (left) $n = 1$, smoothed at R_c, (middle) $n = -1$ smoothed at R_c, (right) $n = -1$, smoothed at $2R_c$. Only one in four grid points in each spatial direction on the 64^3 grid are sampled: 4096 points in all.

Figure 9. Distribution functions for the case $n = -1$, $k_{nl} = 8$, $R_s = R_c$. The N-body results are shown as the solid line; linear, lognormal and Zeldovich approximations are shown as in the key, in straightforward form on the left and with k-space truncation on the right.

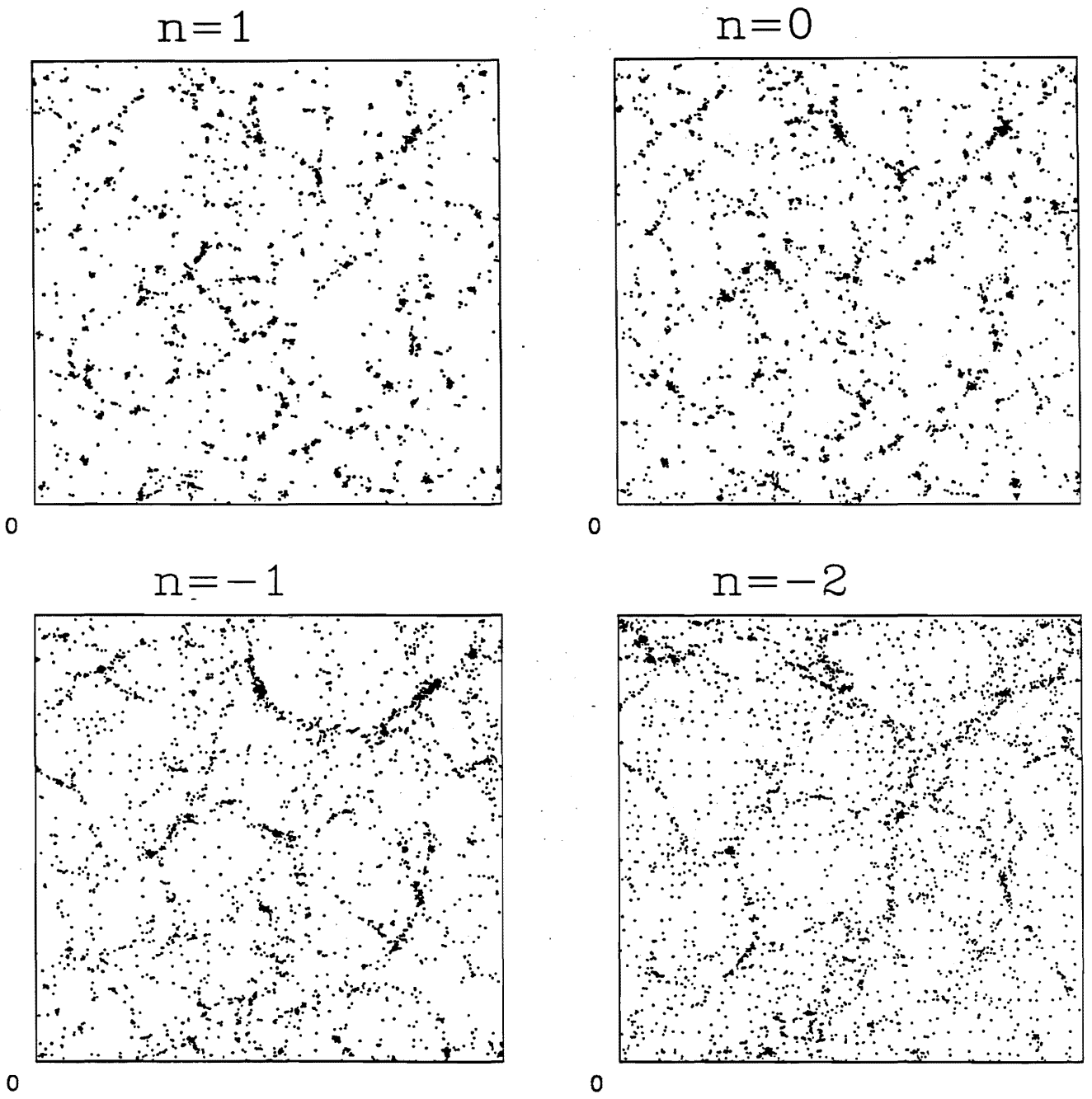

FIGURE]

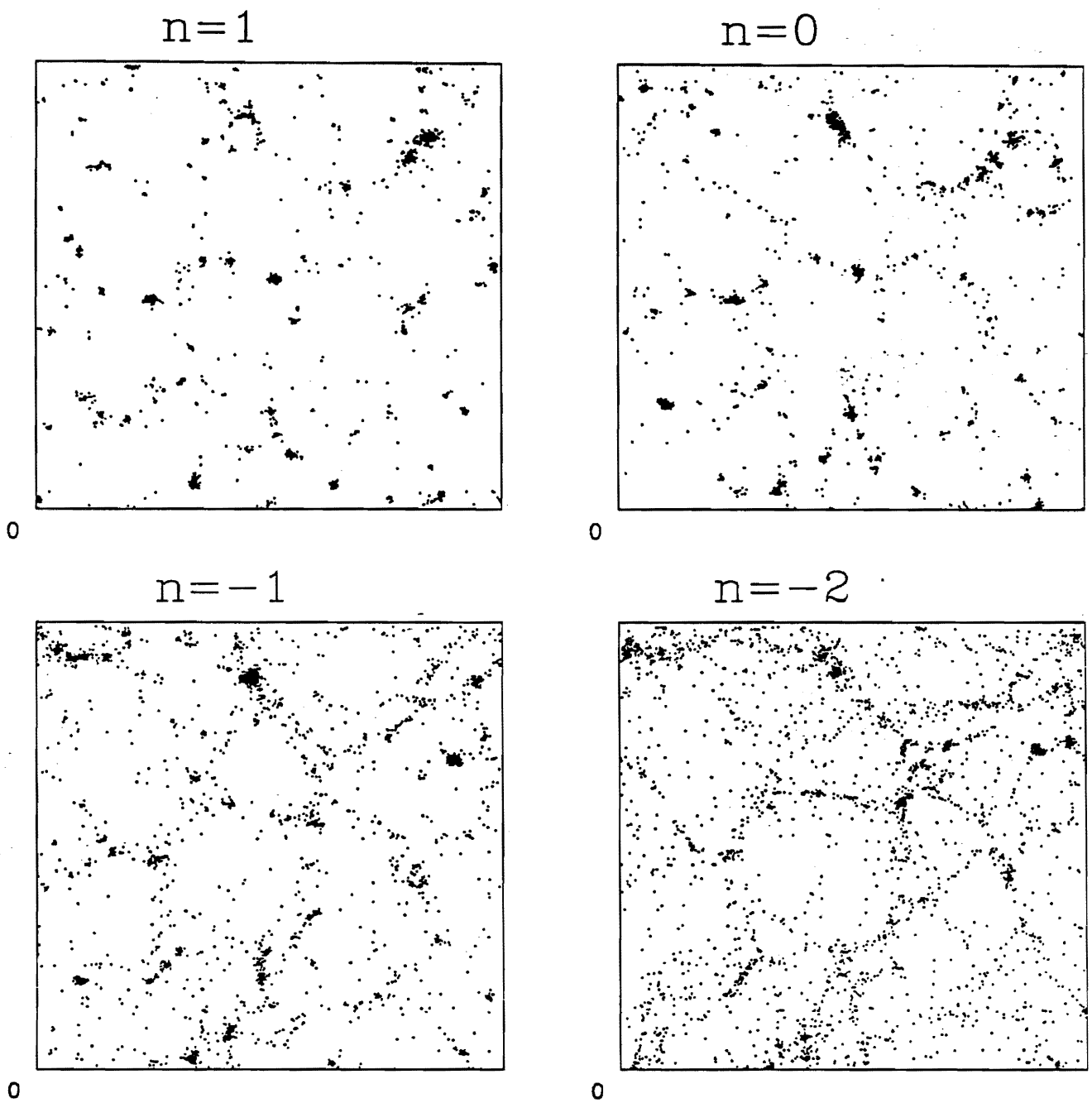

FIGURE 2

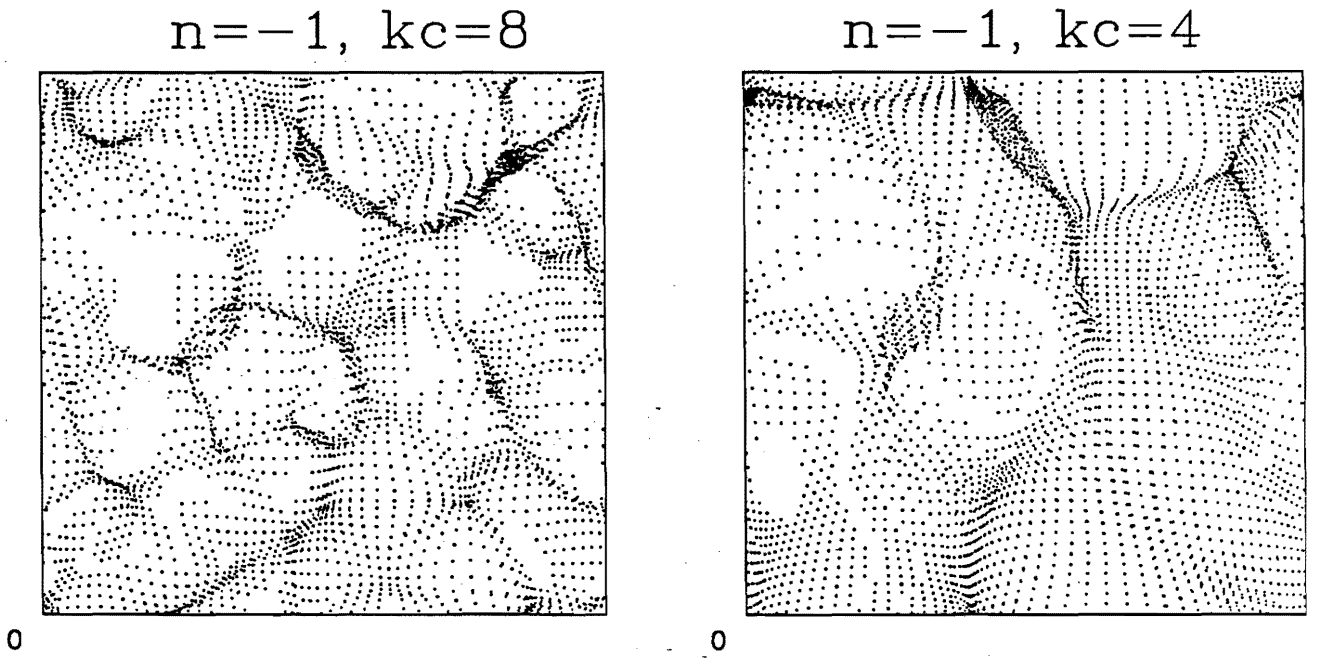

FIGURE 3

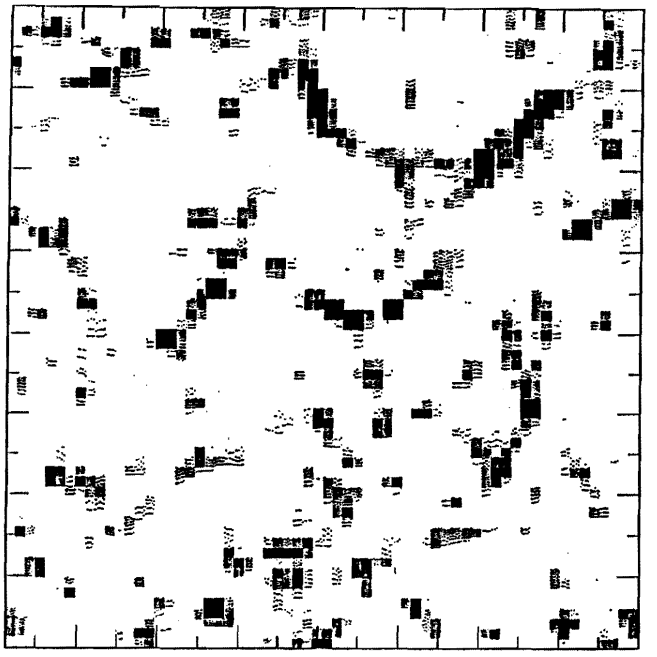

FIGURE 4a

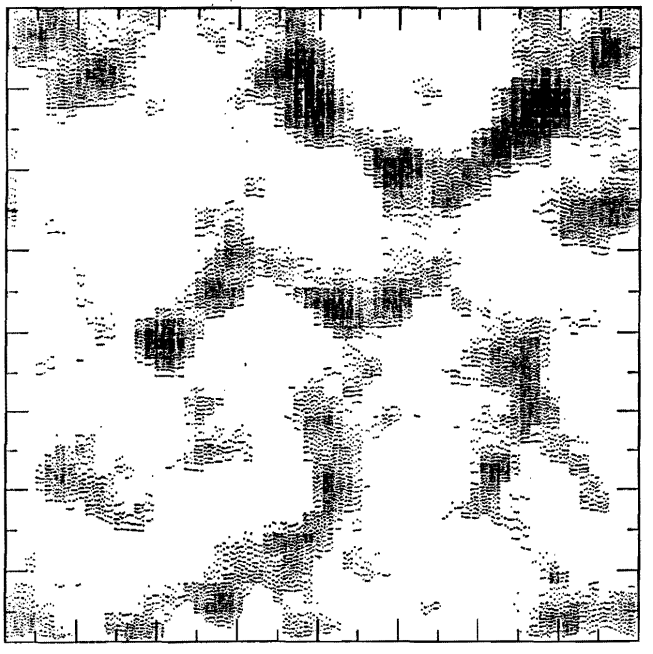

FIGURE 4b

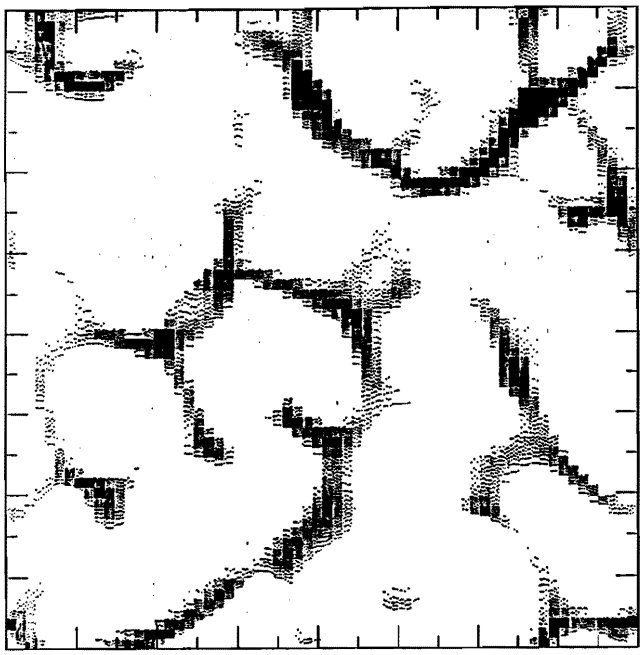

FIGURE 4c

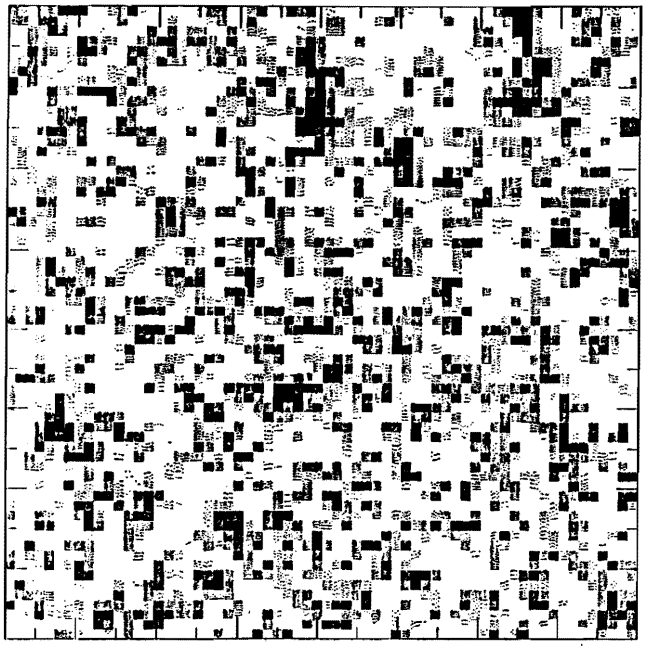

FIGURE 4d

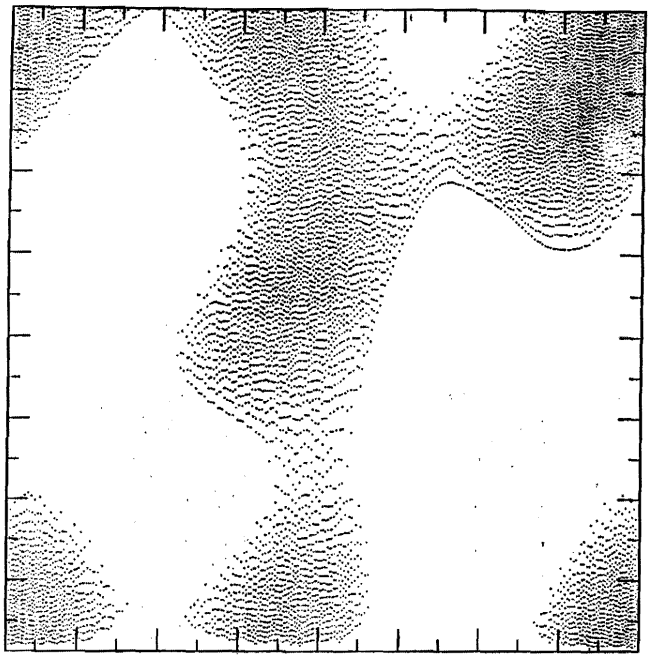

FIGURE 4e

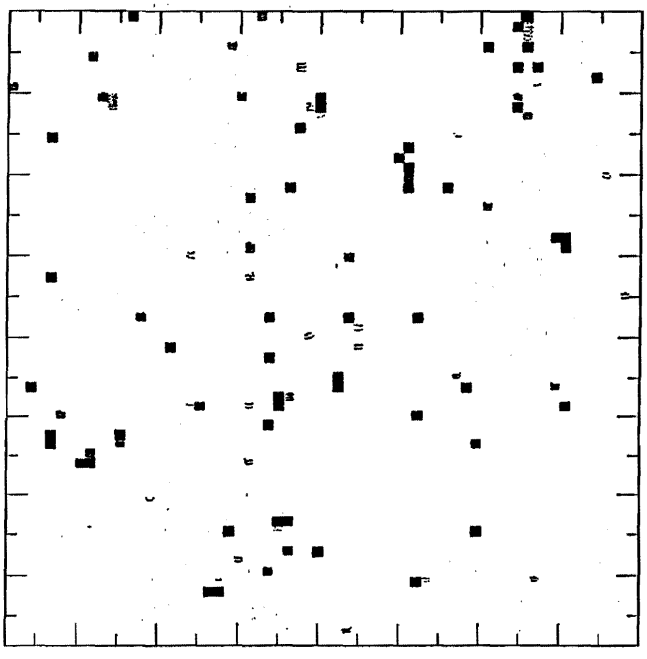

FIGURE 4f

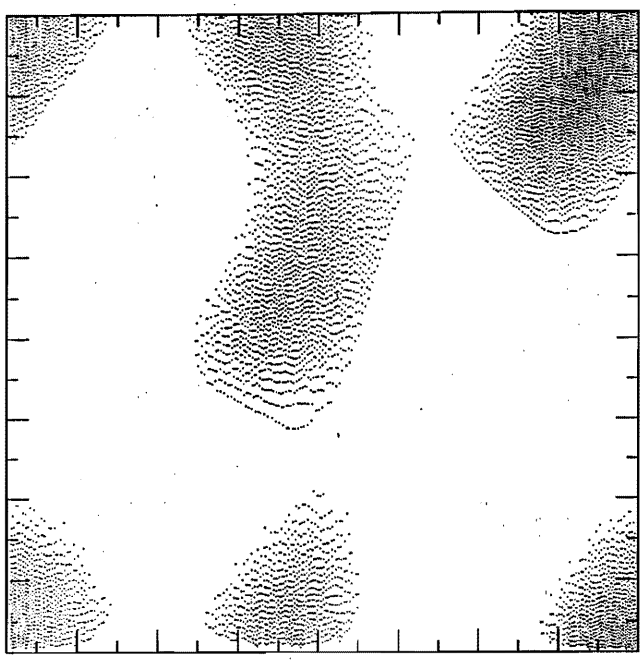

FIGURE 4g

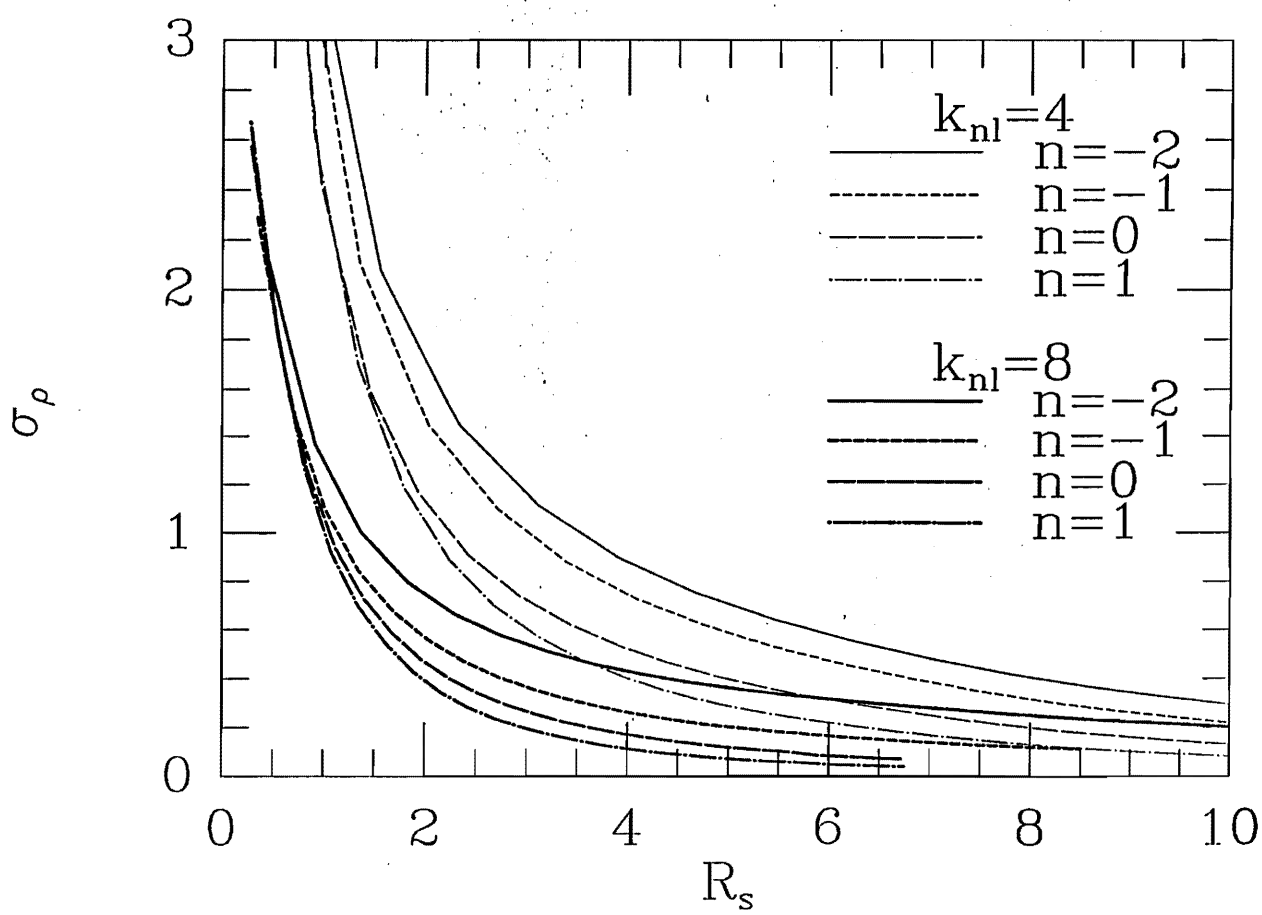

FIGURE 5

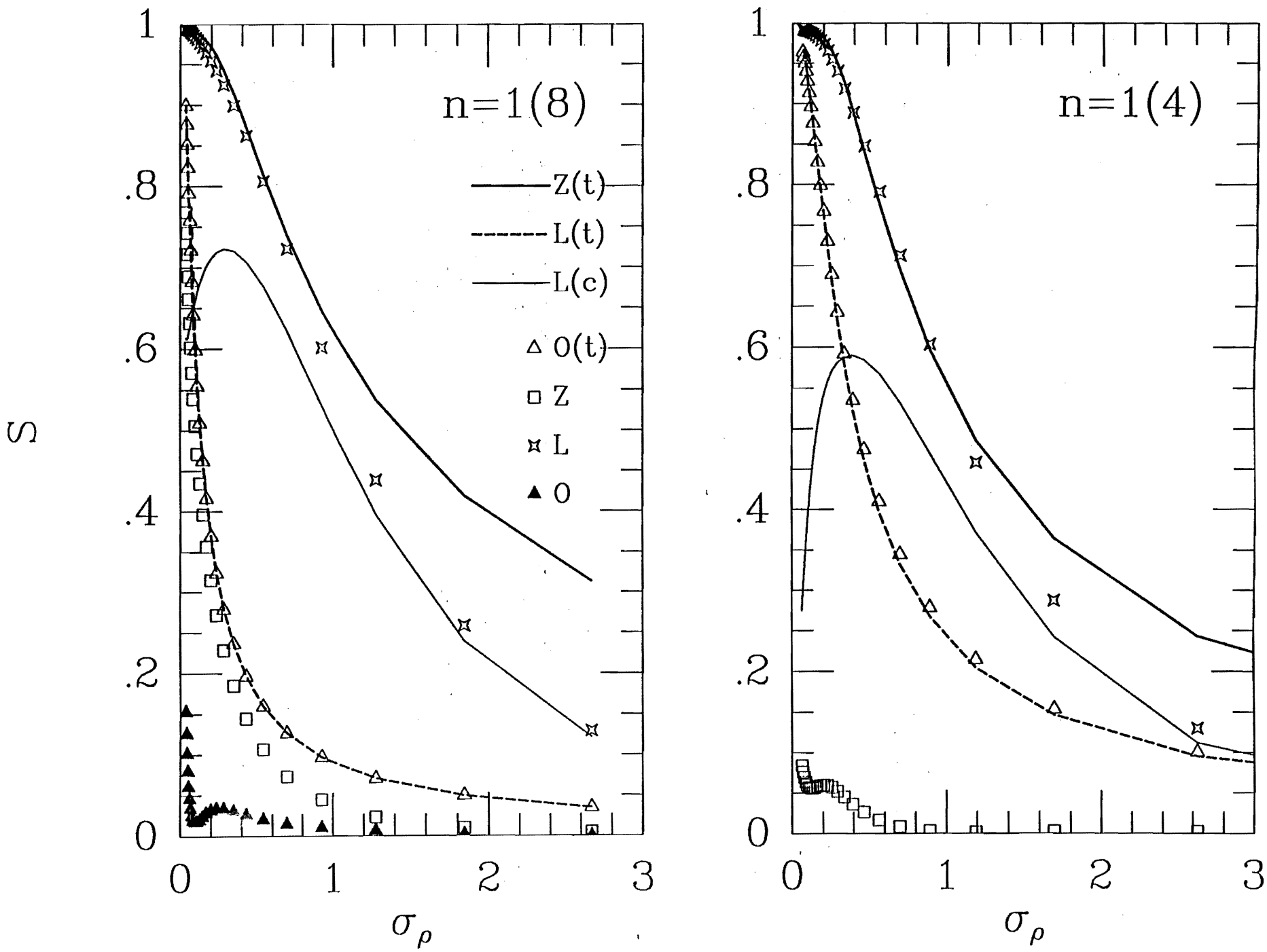

FIGURE 6a

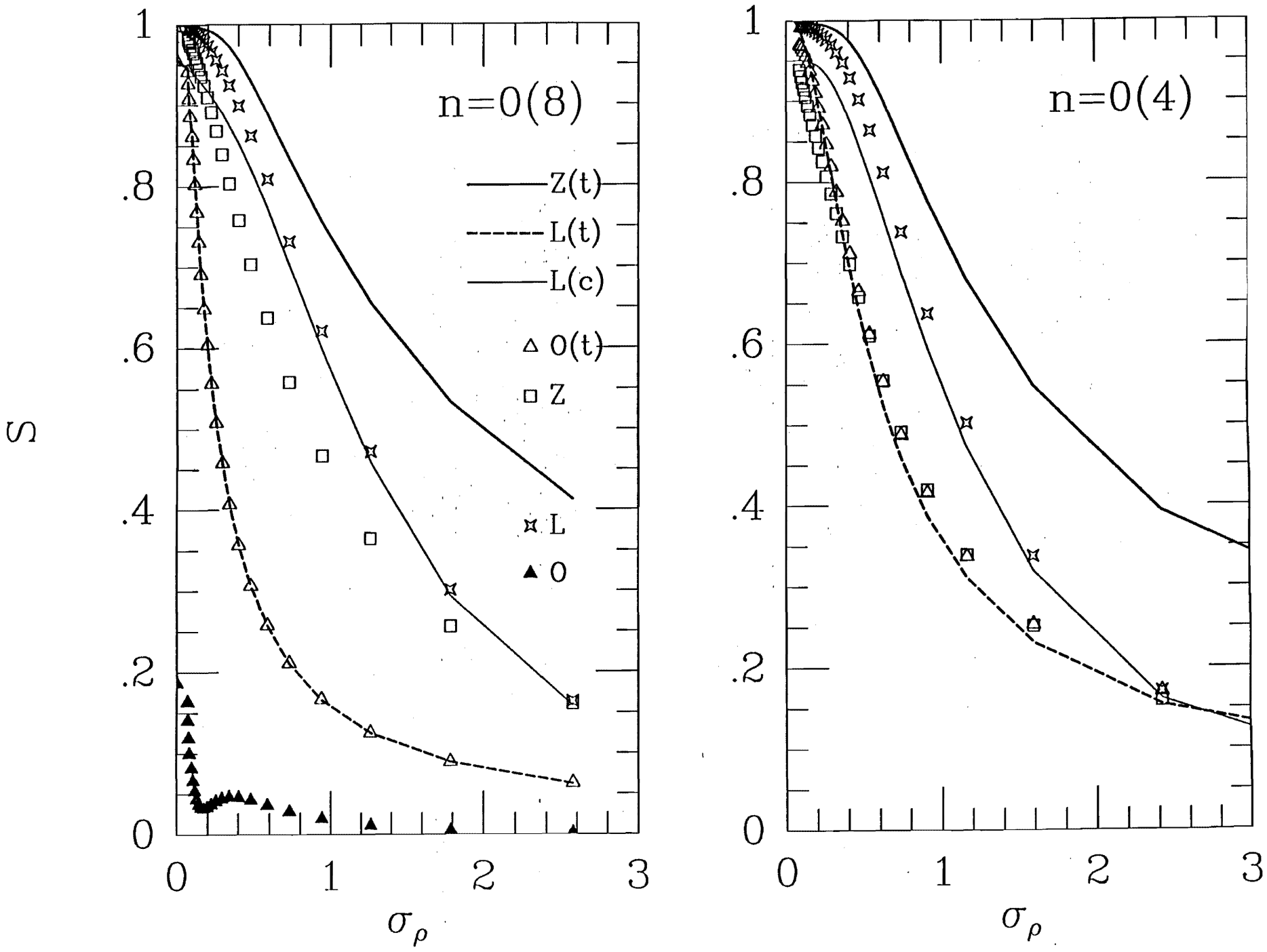

FIGURE 6b

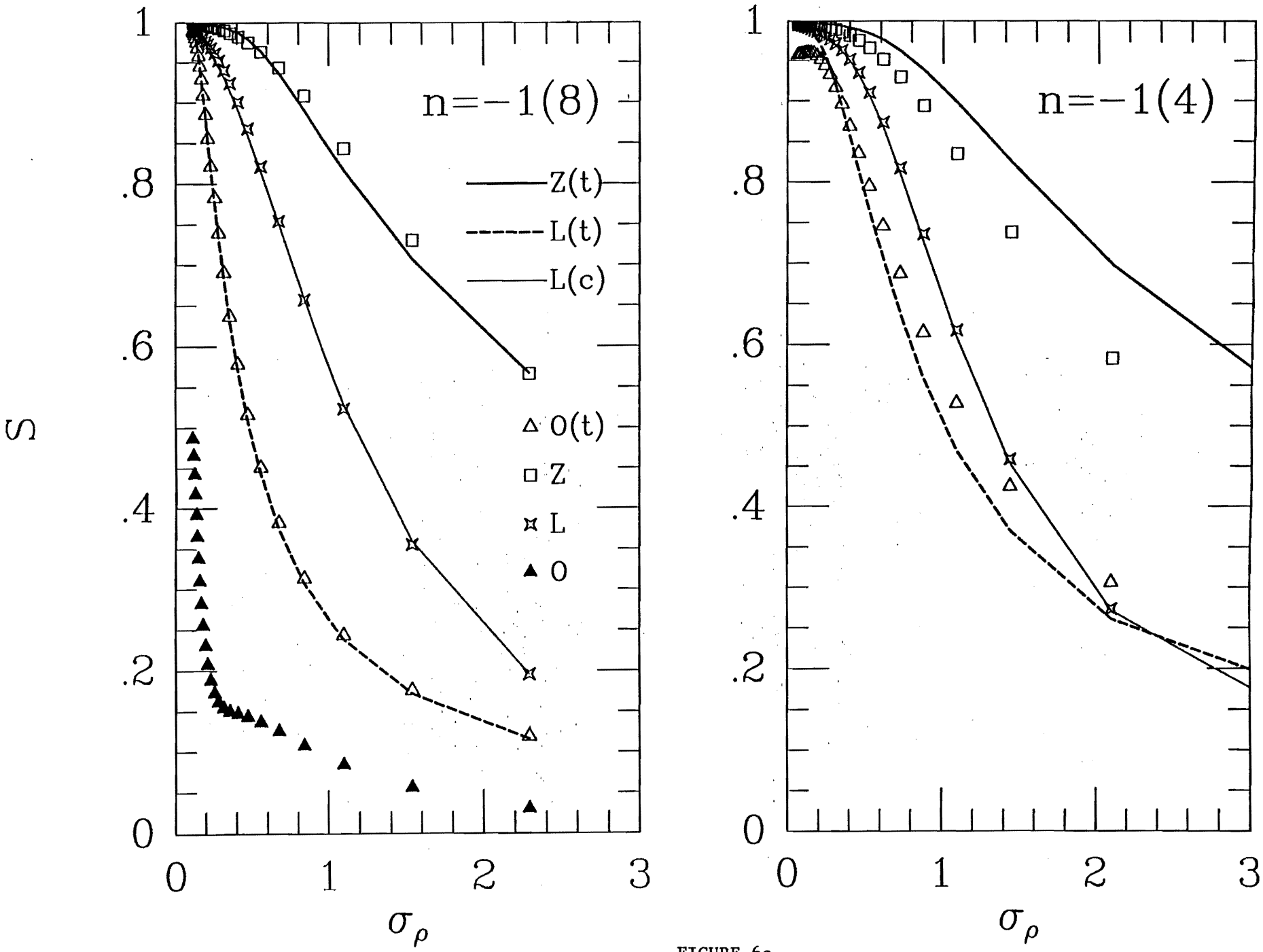

FIGURE 6c

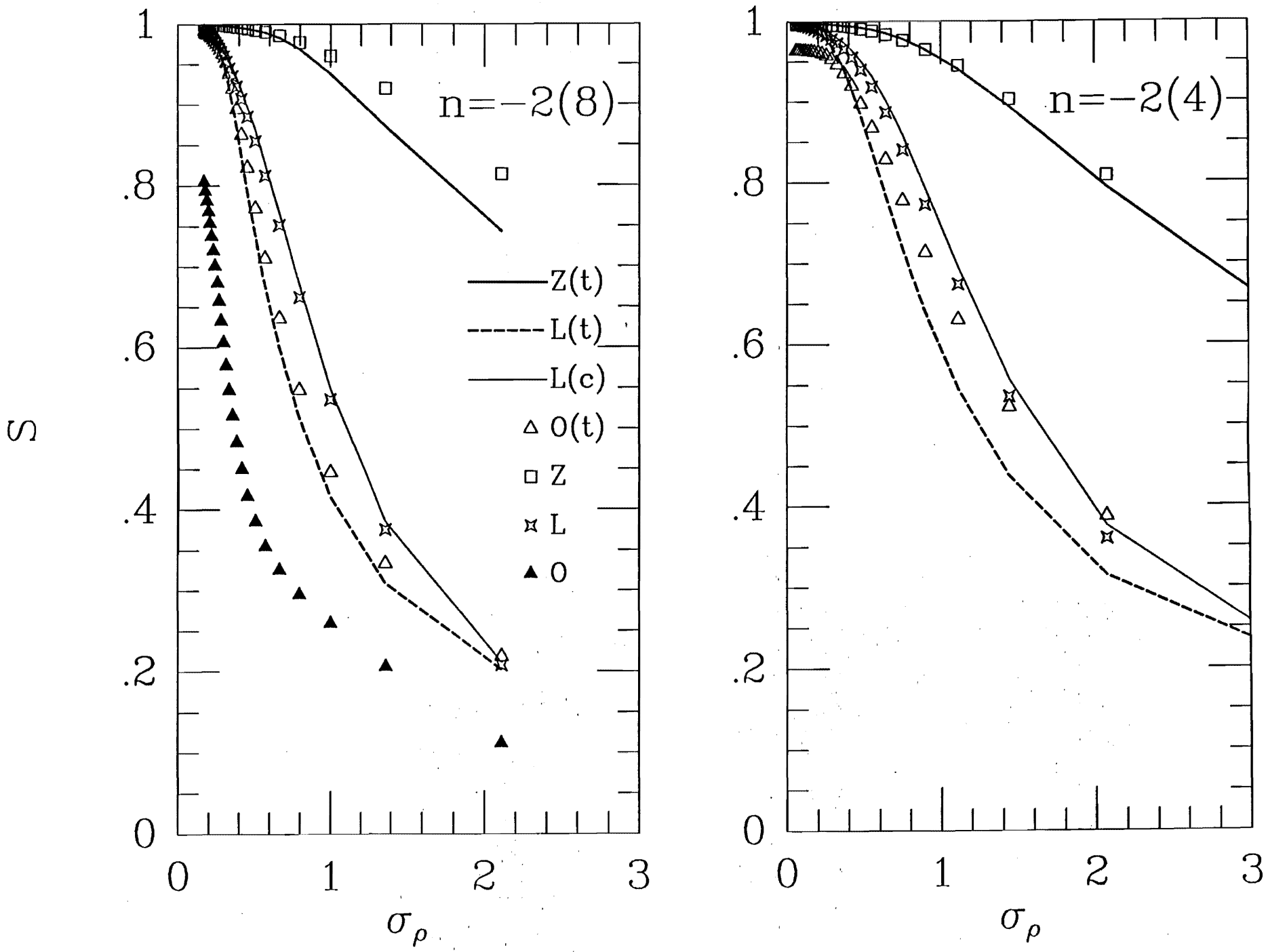

FIGURE 6d

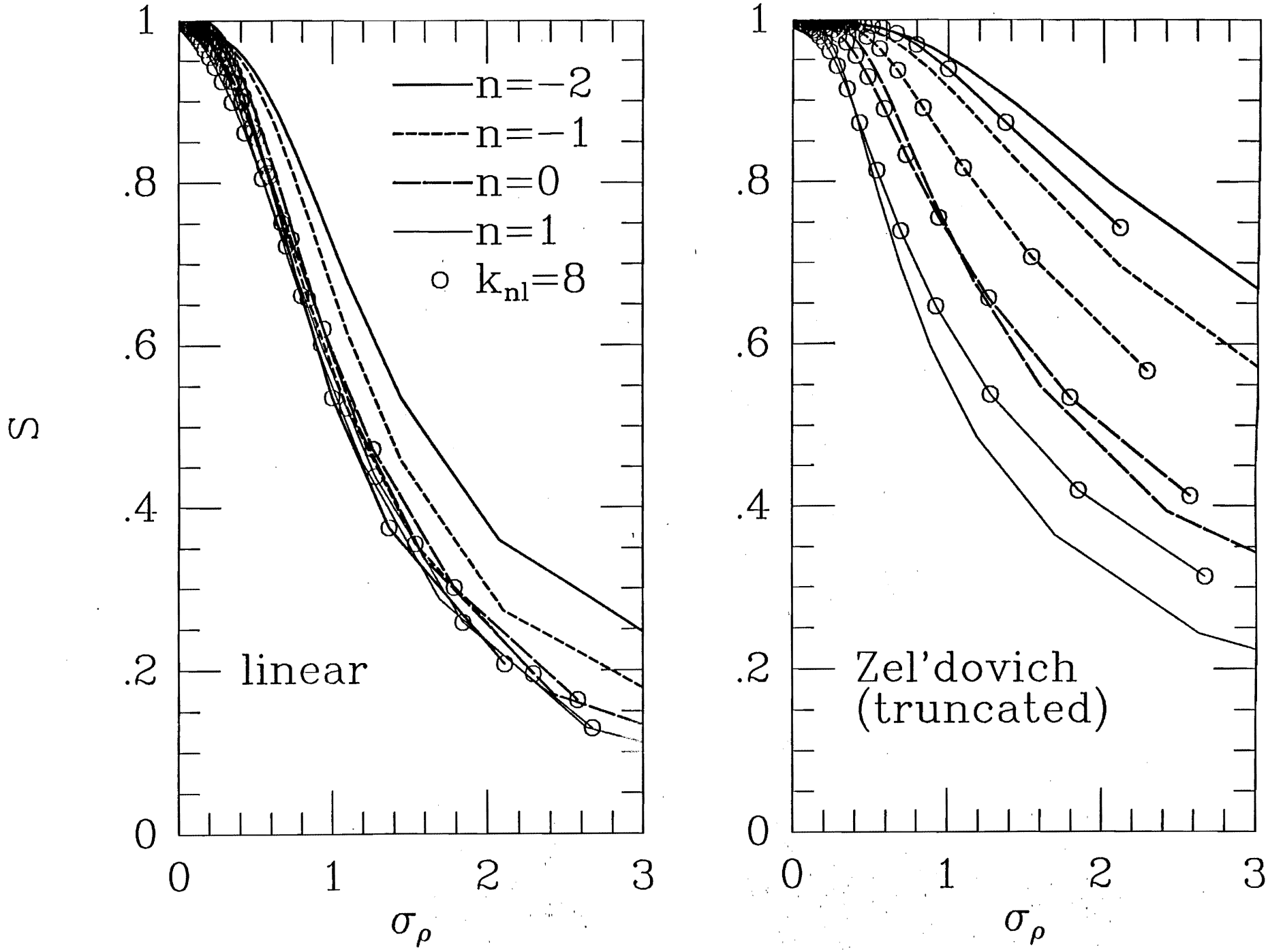

S
1
.8
.6
.4
.2
0
0
1
2
3
σ_ρ
n=−2
n=−1
n=0
n=1
k_{nl}=8
linear
Zel'dovich
(truncated)

FIGURE 7

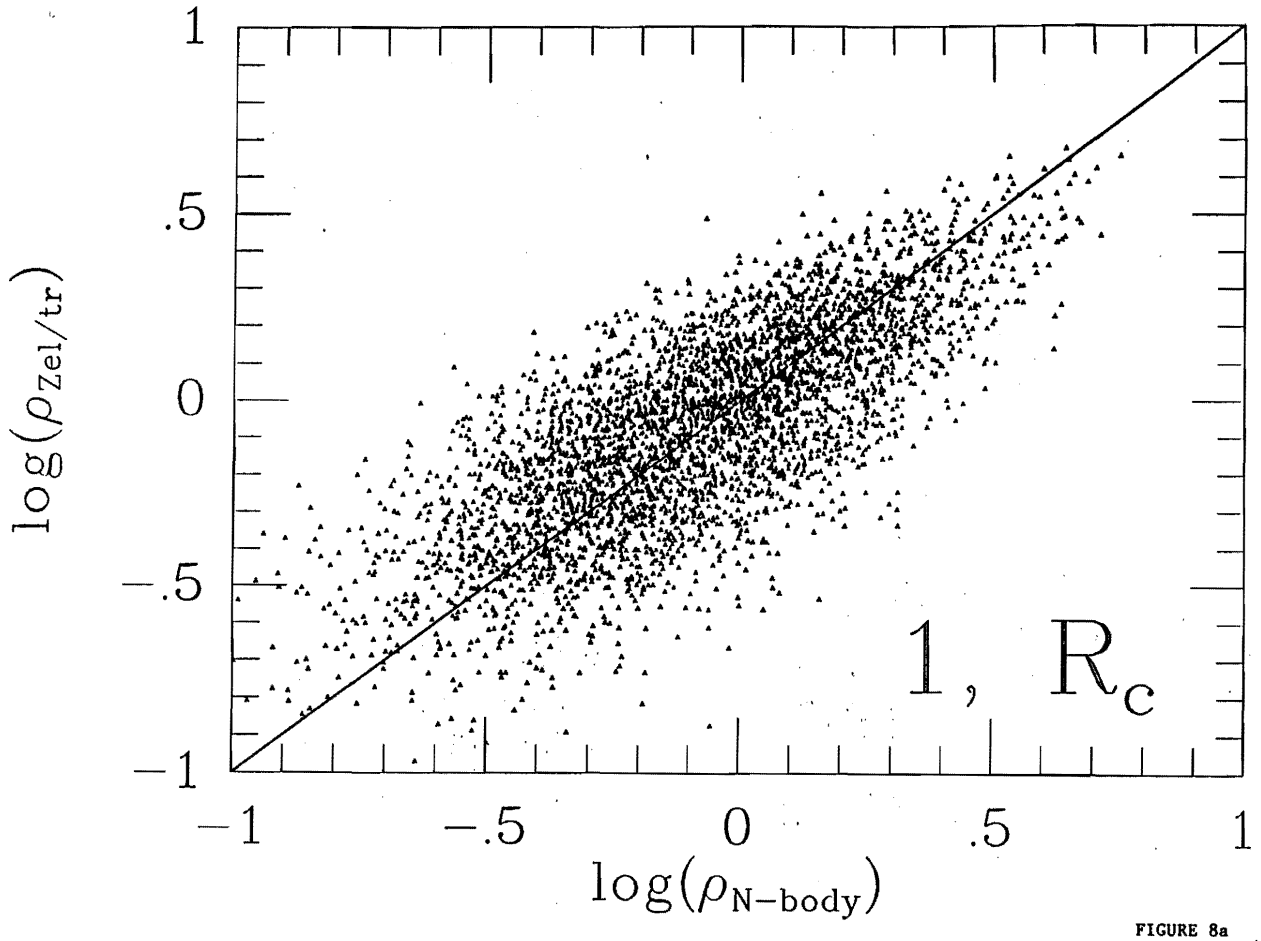

FIGURE 8a

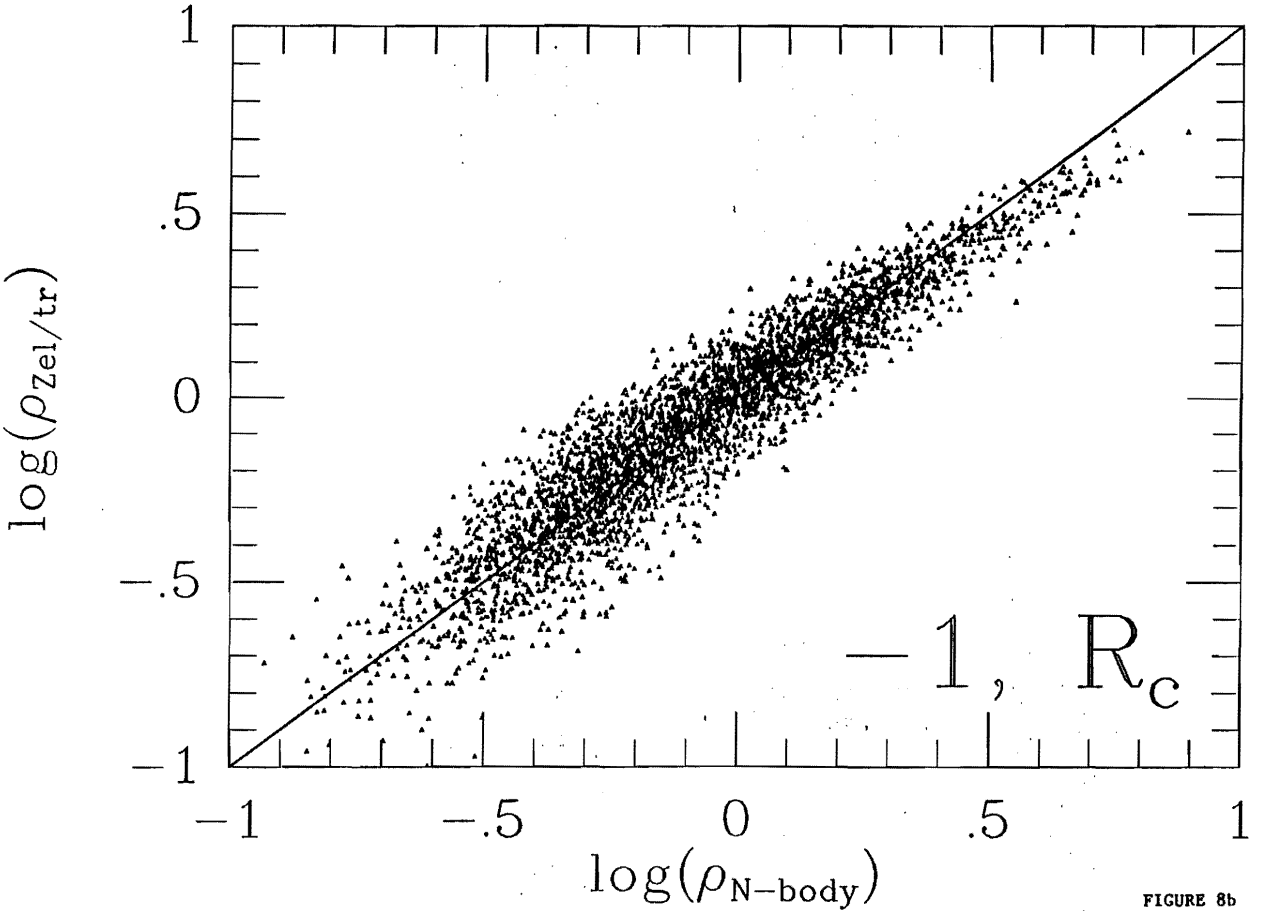

FIGURE 8b

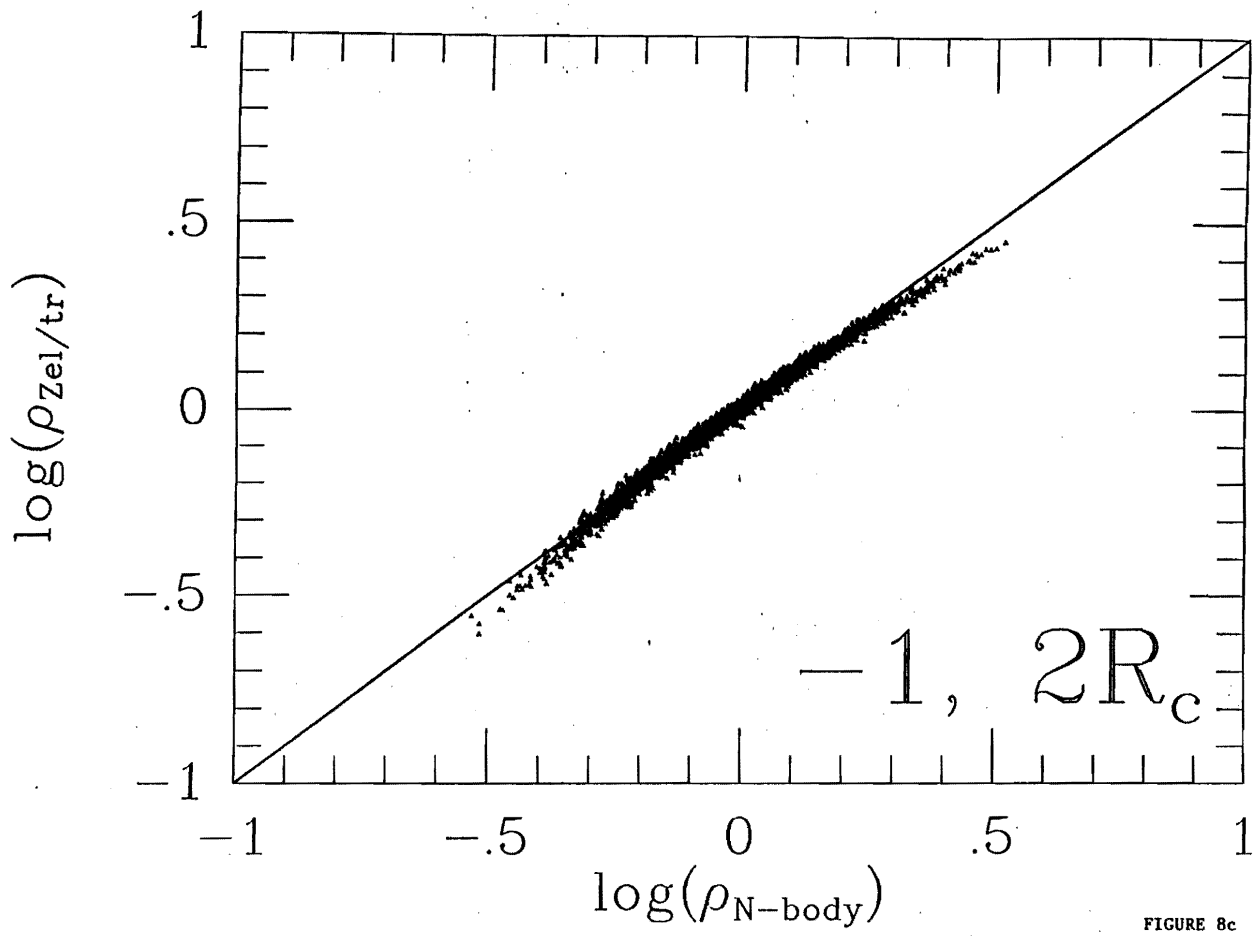

FIGURE 8c

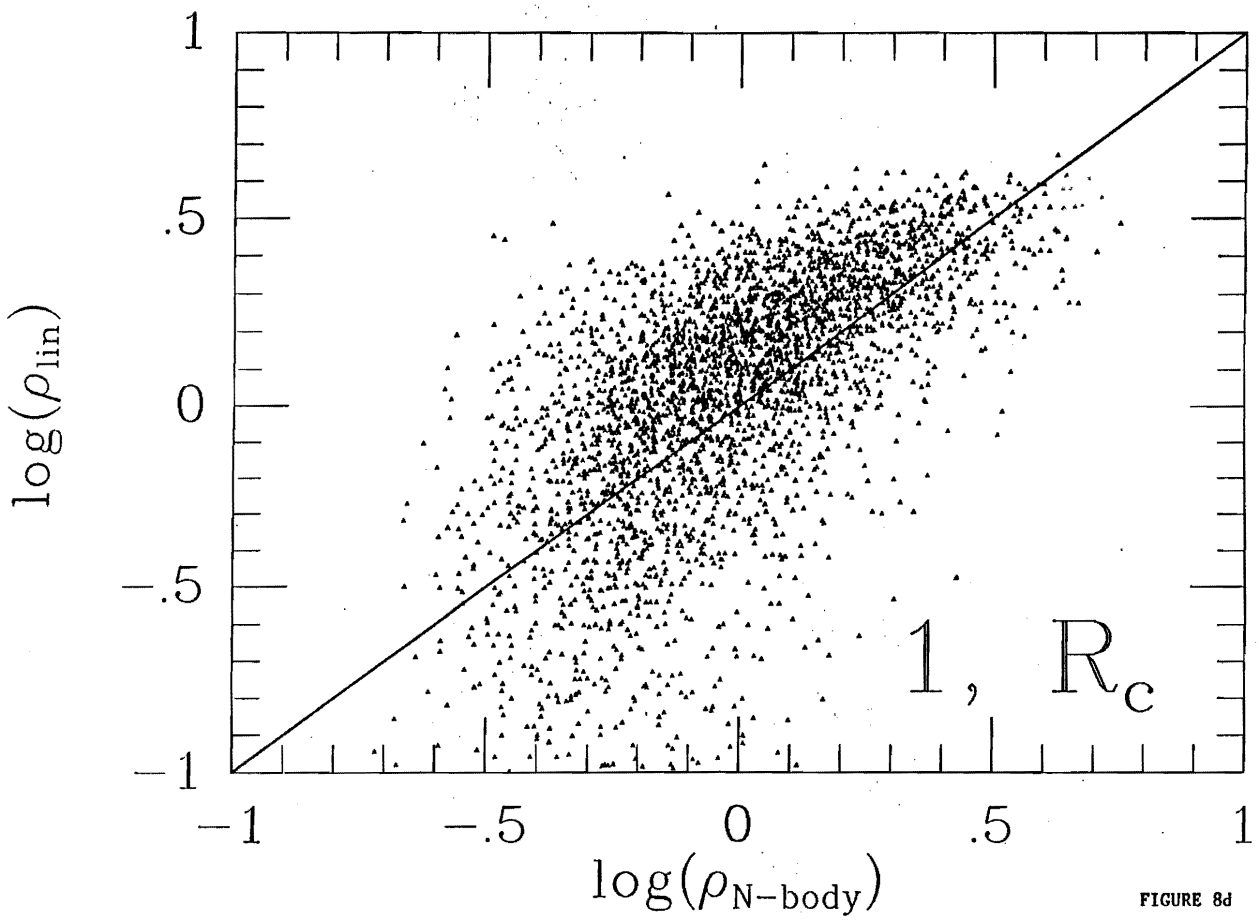

FIGURE 8d

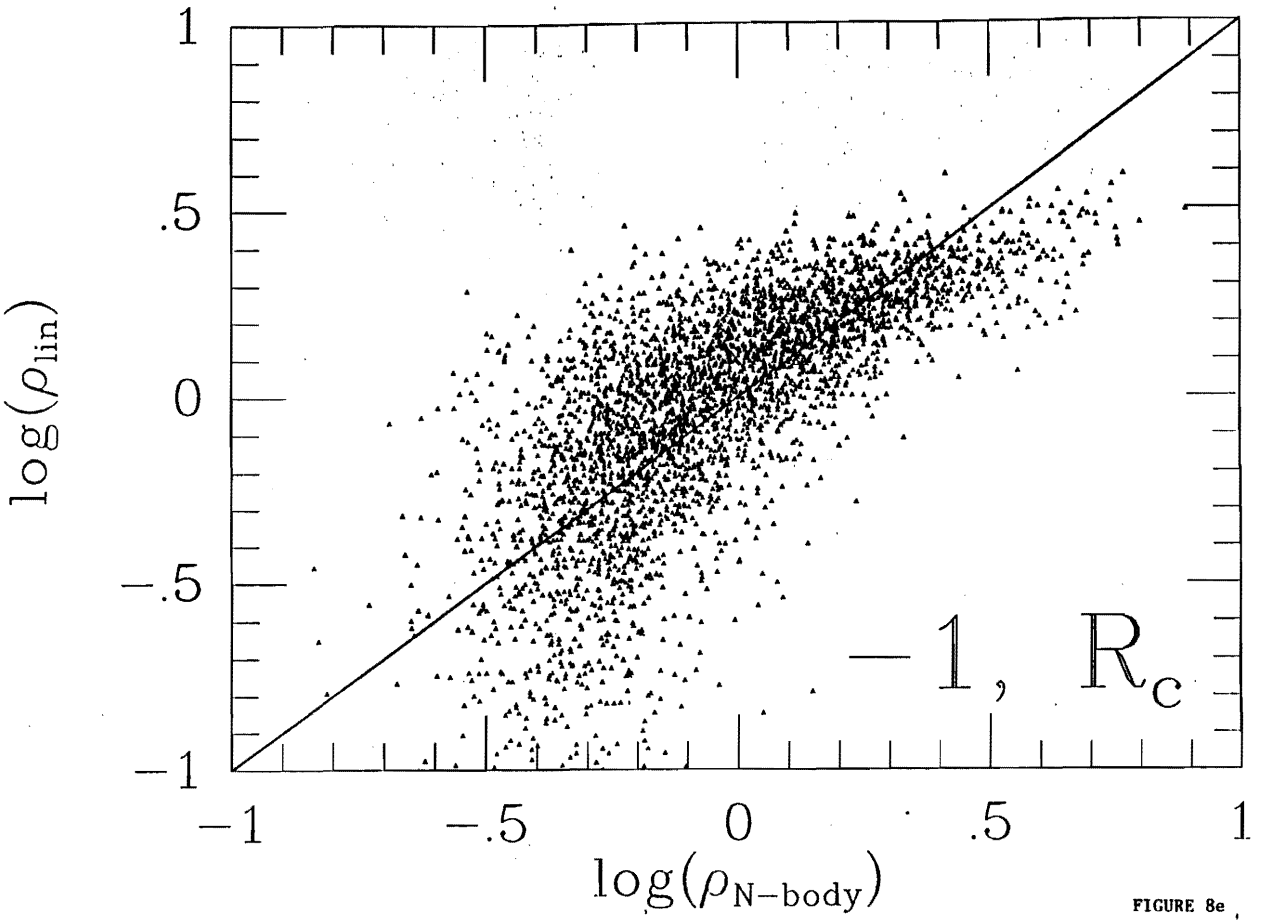

FIGURE 8e

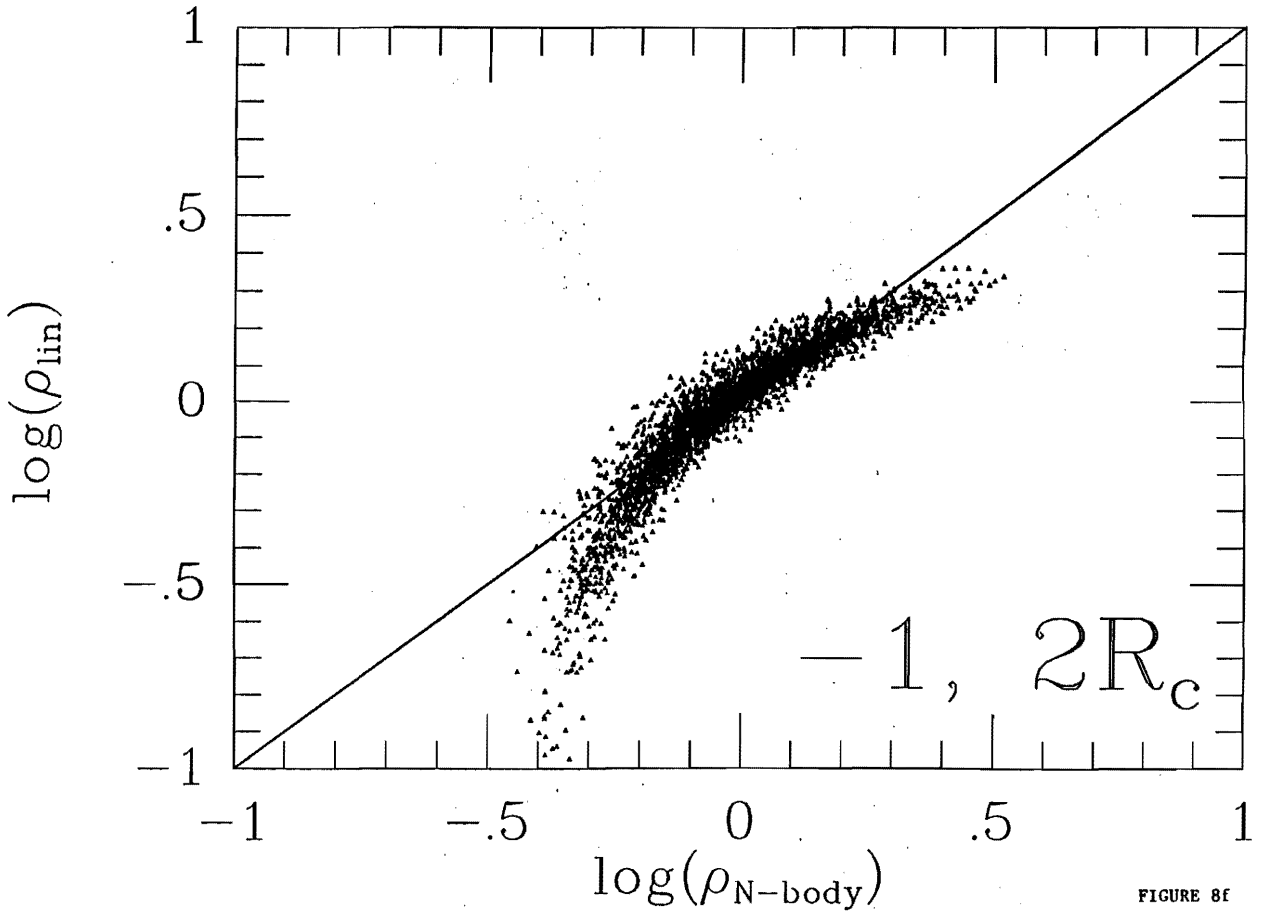

FIGURE 8f

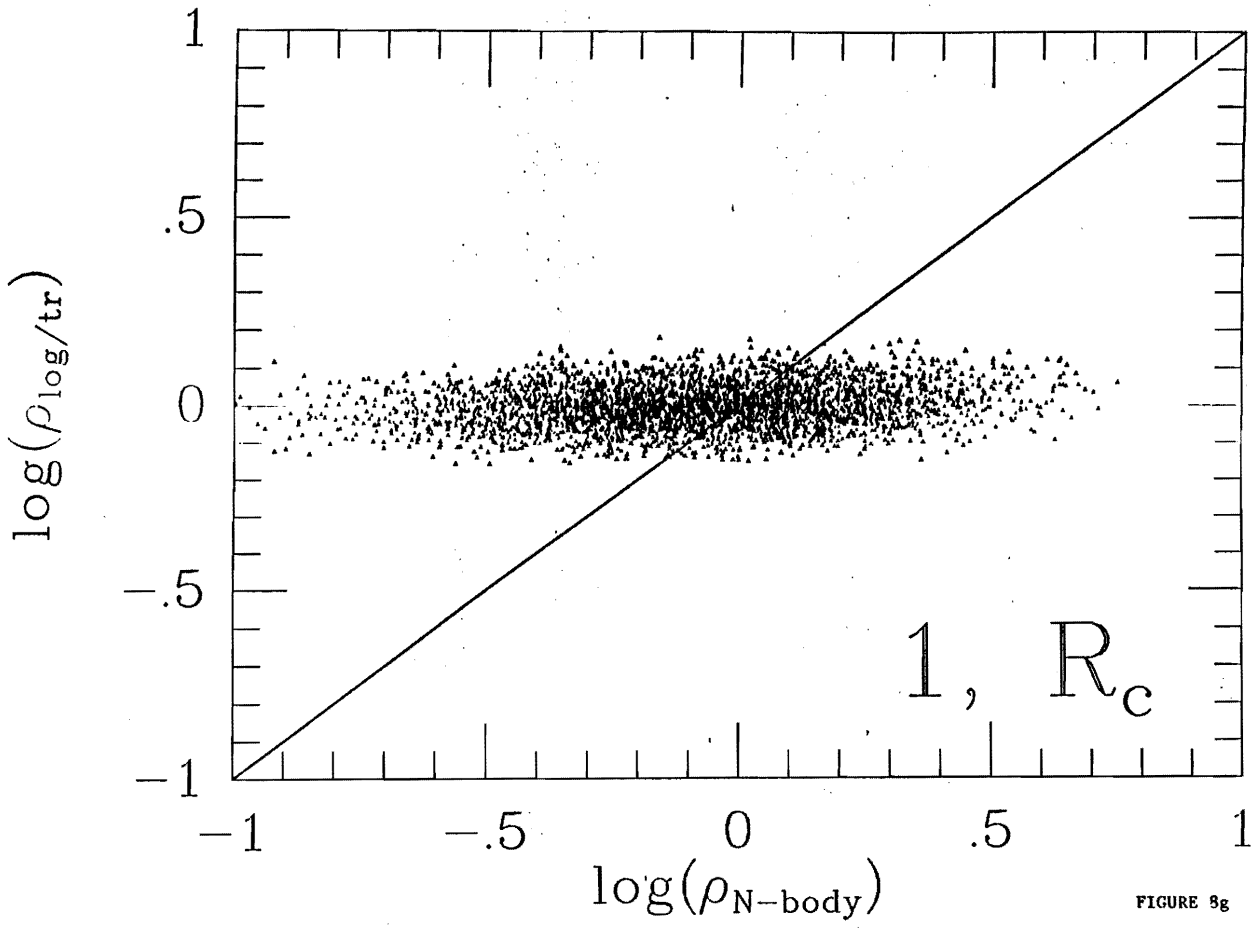

FIGURE 8g

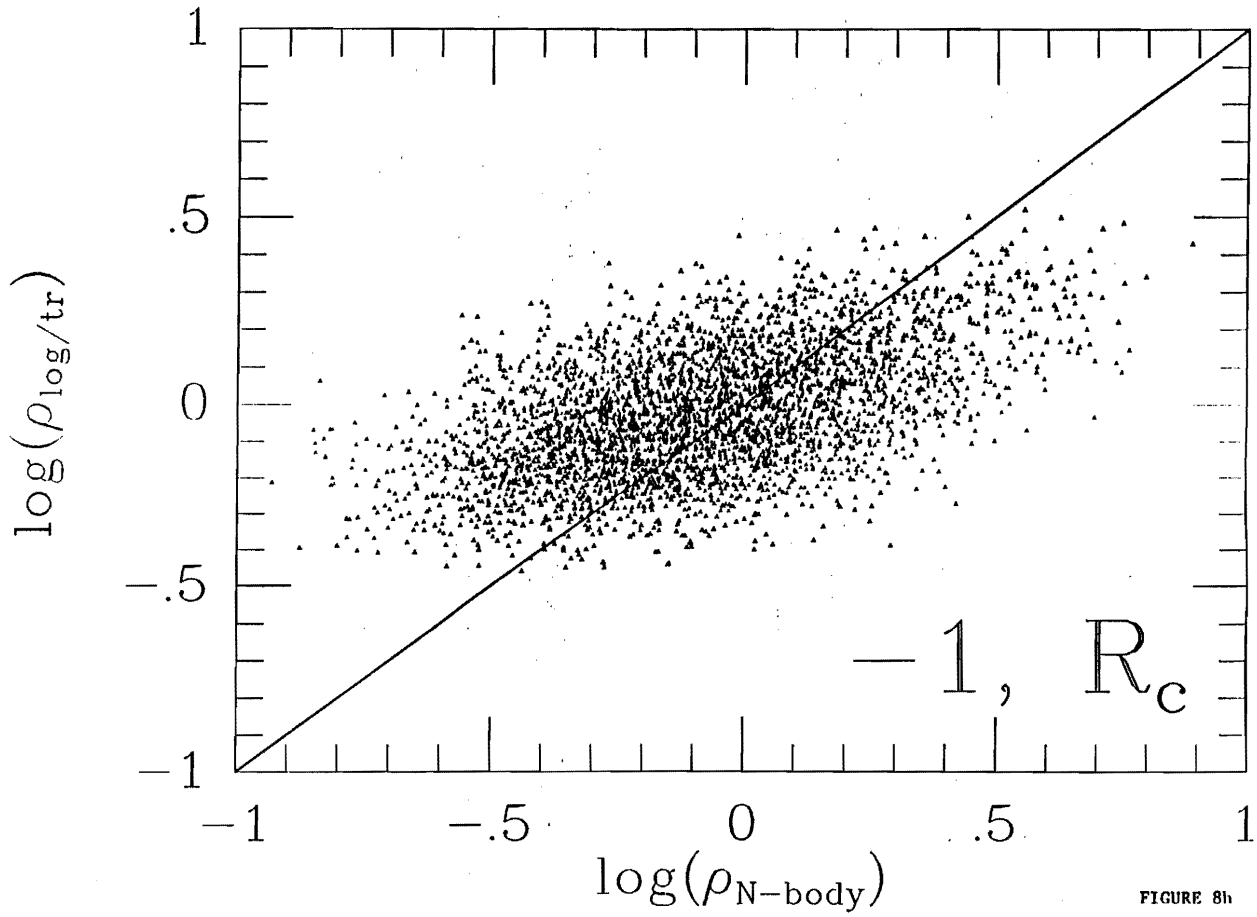

FIGURE 8h

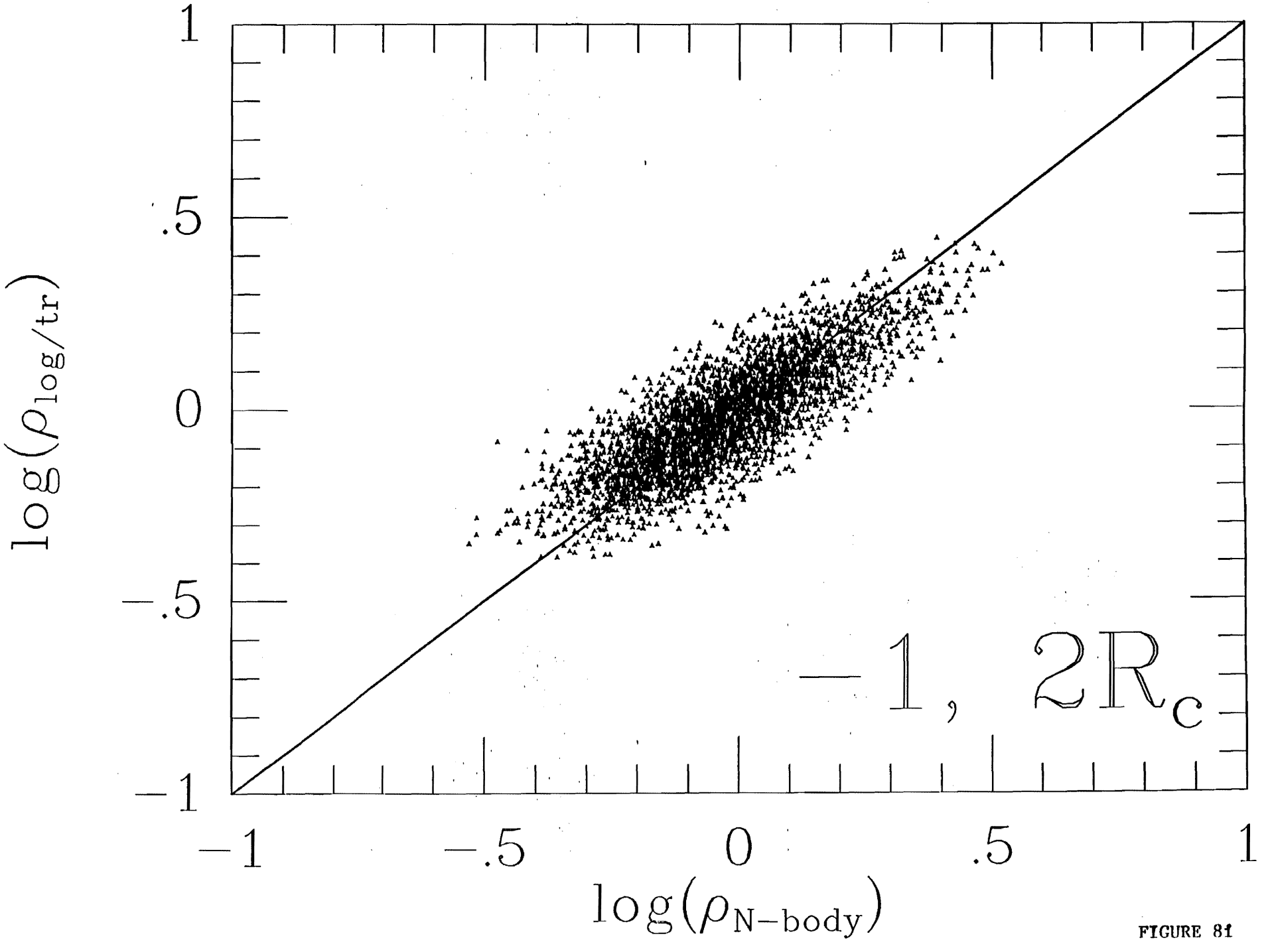

FIGURE 81

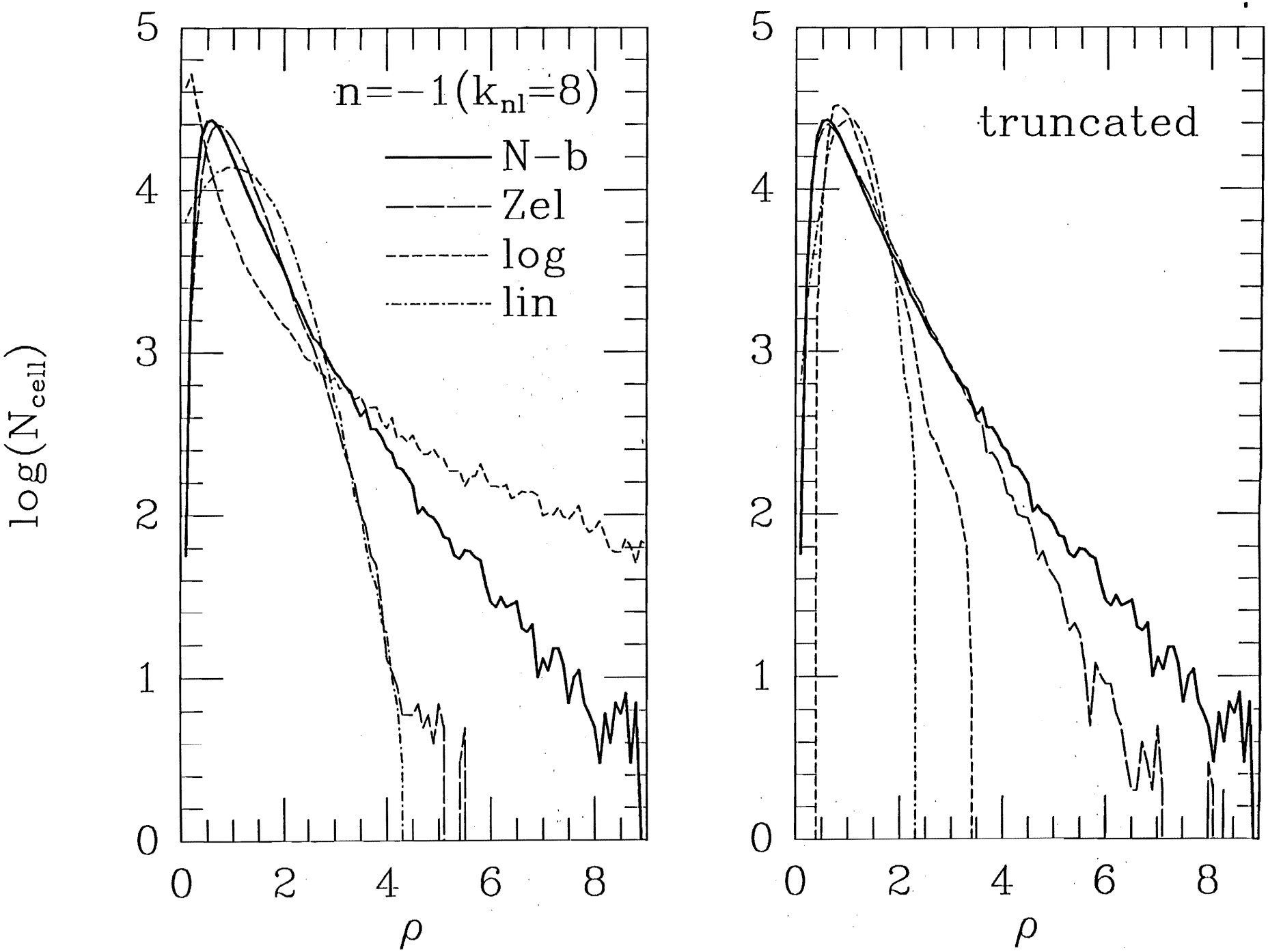

FIGURE 9